International
WOCE
Newsletter

Number 42 ISSN 1029-1725 January 2002

Final Conference

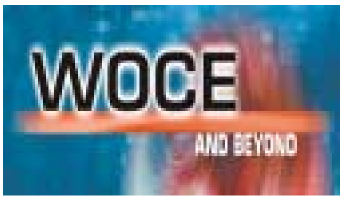

San Antonio
18-22 November
2002

IN THIS ISSUE

News from the WOCE IPO

W. John Gould, Director, WOCE IPO and ICPO, Southampton Oceanography Centre, UK. john.gould@soc.soton.ac.uk

Last but not least

I write this on January 1st 2002, at the dawn of a new year, a day on which we make resolutions and look forward with anticipation to the months ahead. Although this will be WOCE's last year as a part of WCRP, we expect a flurry of activity. The activities in this final year were a focus for the WOCE Scientific Steering Group that met at Scripps Institution in early December. This, the SSG's 28th meeting, had as its main focus an assessment of the progress that WOCE has made towards meeting its objectives. Each SSG member was assigned an area of science and asked to start to assess:

- Where we stood in the 1980s before WOCE started
- What progress had been made since then (and how much of that progress resulted from WOCE)
- What are the limits to further progress?
- What action should WOCE/WCRP take?

These papers covered the topics of

- Large scale air-sea fluxes and their divergences
- Oceanic property transports
- The oceans' dynamic balance and its response to surface fluxes
- Variability and representativeness of the WOCE data set
- Water mass ventilation and circulation rates
- Cost-effective monitoring of the oceans for climate
- Developments in ocean and coupled models

They will be developed and refined and will form the core of the WOCE presentation to the WCRP's Joint Scientific Committee in Hobart in March.

The SSG had a conference call with Carl Wunsch to discuss the programme for the final WOCE Conference "WOCE and beyond". The SSG endorsed the programme (presented on Pages 29 and 30) that had been planned by the

About WOCE

The World Ocean Circulation Experiment (WOCE) is a component of the World Climate Research Programme (WCRP), which was established by WMO and ICSU, and is carried out in association with IOC and SCOR.

WOCE is an unprecedented effort by scientists from more than 30 nations to study the large-scale circulation of the ocean. In addition to global observations furnished by satellites, conventional in-situ physical and chemical observations have been made in order to obtain a basic description of the physical properties and circulation of the global ocean during a limited period.

The field phase of the project lasted from 1990–1997 and is now being followed by Analysis, Interpretation, Modelling and Synthesis activities. This, the AIMS phase of WOCE, will continue to the end of 2002.

The information gathered during WOCE will provide the data necessary to make major improvements in the accuracy of numerical models of ocean circulation. As these models improve, they will enhance coupled models of the ocean/atmosphere circulation to better simulate – and perhaps ultimately predict – how the ocean and the atmosphere together cause global climate change over long periods.

WOCE is supporting regional experiments, the knowledge from which should improve circulation models, and it is exploring design criteria for long-term ocean observing system.

The scientific planning and development of WOCE is under the guidance of the Scientific Steering Group for WOCE, assisted by the WOCE International Project Office (WOCE IPO):

- W. John Gould, *Director*
- Peter M. Saunders, *Staff Scientist*
- N. Penny Holliday, *Project Scientist*
- Mike Sparrow, *Project Scientist*
- Jean C. Haynes, *Administrative Assistant*

For more information please visit:
http://www.woce.org

Scientific Committee. Plenary speakers are now being invited. It promises to be a fitting celebration of WOCE's achievements as well as offering a chance to look into the future. You'll very soon be able to register for the conference at www.WOCE2002.tamu.edu. Just as we did in the 1998 Halifax Conference we encourage you to submit posters demonstrating the contribution that you made to WOCE.

WOCE Atlases

All of the WOCE Atlas Principal Investigators met before the SSG so that they could review progress and resolve outstanding problems. I am pleased to tell you that we are on track for one (and perhaps even two) volumes to be ready for launch at the Conference. This is an exciting and challenging venture requiring a great deal of hard work by many people. The outcome will be the definitive ocean atlases for many years to come.

WOCE Data matters

In November representatives of the WOCE data centres and members of the WOCE Data Products Committee met in Delaware. They resolved issues that will lead to the final version (V3) of the WOCE data sets, which will be a much more "integrated" product than earlier versions. A key step is ensuring that all data centres use a uniform set of variable names and units. This will result in a data set in which one can extract a variable (say temperature) from a number of data streams (e.g. CTDs, current meters, and XBTs).

To match this data set there will be a "WOCE Comprehensive Field Programme Description". This document will be a detailed hardcopy and electronic summary of the field programme (1990-1998 and some pre-WOCE hydrography). It will summarise what was measured, where, when and by whom and will effectively be a complement to the 1988 Implementation Plan. It will contain maps and tables of each aspect of the field programme. Only components that were completed and data submitted by mid-2002 will be included, thus it will also be a description of the final WOCE data set as issued on the Version 3.0 of WOCE Global Data.

Some sections of the document (current meter, sea level, upper ocean thermal, drifters, floats) are already complete . The data streams that derive from the hydrographic programme (WHP One-time and Repeats, ADCP, and Surface Met) are yet to be completed.

A remaining challenge is to find the approximately $14,000 that will be required to print and distribute the 2500 copies. If any organisation is willing to contribute to the funding of this venture we will be happy to hear from them.

And finally, looking beyond WOCE, my visit to Scripps gave me an opportunity to talk to Jim Swift who directs the WOCE Hydrographic Programme Office. We discussed safeguarding hydrographic data from sections that have been worked since WOCE ended. These will be of importance to CLIVAR. The WHPO was mandated to process US post-WOCE sections and will now broaden this to include non-US data. A list of key sections is being compiled by the International CLIVAR Project Office and will be passed to the WHPO.

So you see that although 2002 will be the last year of WOCE it will be one of great activity. The WOCE IPO send you all good wishes for the coming year.

Meridional overturning in the North Atlantic

Rick Lumpkin and Kevin Speer,
Department of Oceanography, Florida State University, USA.
Rlumpkin@ocean.ocean.fsu.edu

Across 11°S in the Atlantic Ocean, the northward flow of surface water, Antarctic Intermediate Water (AAIW) and Antarctic Bottom Water (AABW) is compensated by the southward flow of North Atlantic Deep Water (NADW). Diapycnal transformation, including surface fluxes and interior mixing, closes this meridional overturning circulation (MOC) pattern. Thus, if our knowledge of absolute isopycnal fluxes across 11°S and air-sea heat and freshwater fluxes in the North Atlantic is sufficient to be able to resolve the above errors we can estimate the density distribution of subsurface mixing. A minimal-mixing solution, achieved by small adjustments to the initial 'level of no motion' and heat fluxes, requires little to no subsurface mixing in density classes of the subtropical thermocline. Significant mixing must balance the air-sea driven buoyancy gain of equatorial surface water and the large-scale convergence of bottom water (AABW and Nordic Seas Overflow Water, NSOW) (Speer, 1997).

This approach determines the basin-scale distribution of surface and subsurface diapycnal transformation. For gyre-scale resolution, the box inverse model technique (c.f. Wunsch, 1996) can be applied to zonal hydrographic sections. At subpolar latitudes this technique has been limited by the large volume of outcropping water exposed to intense diapycnal transformation. Previous models typically terminate at the subtropical-subpolar boundary, or group all outcropping water masses into a single model layer. Here we present results from a box inverse model of the North Atlantic which explicitly includes air-sea forcing on outcropping layers and can thus resolve surface diapycnal transformation in Subtropical and Subpolar Mode Water classes. Using the Gauss-Markov estimation, the model adjusts reference velocities, corrections to the air-sea heat and freshwater fluxes and subsurface diapycnal fluxes in order to conserve volume, salinity anomaly and potential temperature in layers defined by neutral density γ^n (Jackett and McDougall, 1997). This approach is generally capable of producing solutions with smaller diapycnal mixing than one would obtain from the isopycnal convergences/ divergences of independent hydrographic section analyses. We seek minimal estimates of interior mixing compatible with hydrographic and surface flux observations, together with the associated various property transports.

The inverse model

The model geometry is shown in Fig 1. Hydrographic sections from WOCE run along nominal latitudes 11°S, 25°N, 46°N, 56°N and additionally close to the Denmark Strait and Mediterranean outflow regions. A composite section was constructed from NANSEN (North Atlantic Nordic Seas Exchanges) and VEINS (Variability of Exchanges in the Northern Seas) hydrographic casts which run from Iceland to the Faroe Islands along the Iceland-Faroe Rise, across the Faroe Bank Channel to the Faroe Bank, then along the Wyville-Thompson Ridge to the Hebridean Shelf off Scotland.

Layer interfaces are defined such that each layer contains an equal volume of the global distribution of γ^n. Air-sea heat and Evaporation-Precipitation fluxes are from UWM (University of Wisconsin-Milwaukee)/COADS (Comprehensive Ocean-Atmosphere Data Set) (da Silva et al., 1994), river fluxes from the GRDC (Global Runoff Data Centre) (Dornblut et al., 1998), and Ekman transports from SOC (Southampton Oceanography Centre) COADS winds (Josey, et al., 2001). The solution is constrained to meet net meridional salt and freshwater fluxes

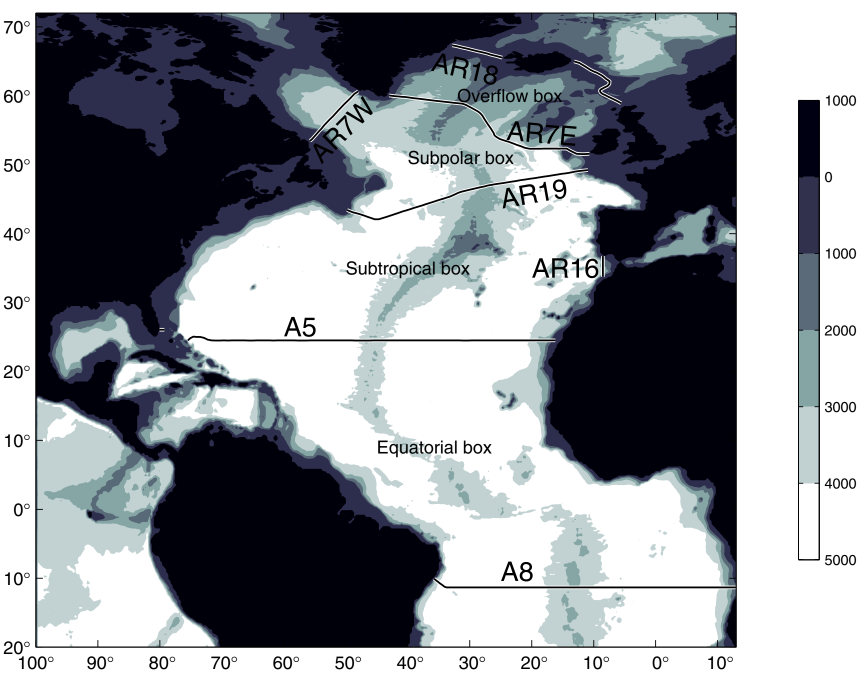

Figure 1
Geometry of the box inverse model, superimposed on bathymetry (metres).

Figure 2
Schematic North Atlantic meridional overturning in the inverse model. Parcel trajectories are presented in model layer (constant γ^n) coordinates, with layer interfaces indicated by horizontal lines. Layers exposed to significant surface forcing are lightly shaded; those below topography are heavily shaded.

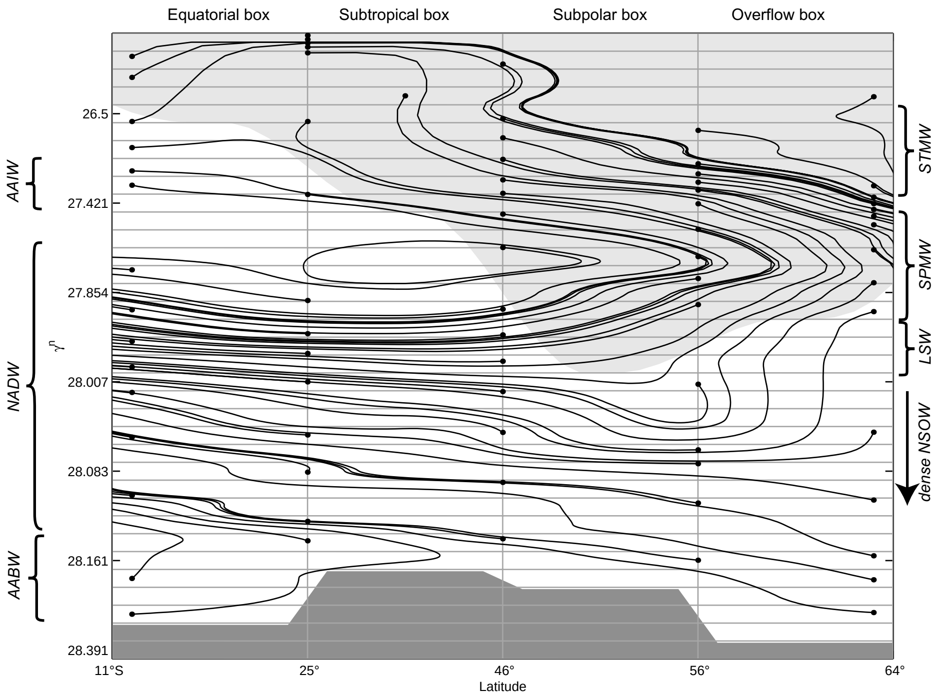

(Wijffels et al., 1992), water mass exchanges with the Nordic Seas (Mauritzen, 1996; Hansen et al., 1999), the net volume flux through the Gibraltar and Florida Straits (Schott et al., 1988), and layer volume transports in the Denmark Strait Channel (Ross, 1984, Girton et al., 2001), the Faroe Bank Channel (Saunders, 1990; Price et al., 2001), the East Greenland and Irminger Currents (Bersch, 1995, Bacon, 1997), the Labrador Current (Lazier and Wright, 1993), and in AABW layers into the North Atlantic (Hall et al., 1997), (Mercier, Speer, 1998).

Results

A model solution closed the volume, salinity anomaly and potential temperature budgets to the desired tolerances within the *a priori* range of reference velocities, air-sea flux corrections and internal mixing (others are discussed in (Lumpkin and Speer, 2002)). At 11°S, the net strength of the MOC is 15.0±2.4 Sv. Fig. 2 is a visualisation of the overturning streamfunction as it appears in the model solution. The figure was created by smoothly interpolating the iso- and diapycnal volume fluxes (total, including geostrophic, Ekman, air-sea and internal mixing components) between each spanning zonal section or section pair. "Parcels" were released on each zonal section, with a vertical distribution determined by the isopycnal transport across that section (i.e. parcels were released where the transport is large). Their trajectories were calculated from the smoothed volume flux field until they left the North Atlantic, either across 11°S or over the Greenland-Iceland-Scotland ridges at nominal latitude 64°N. Diapycnal fluxes within the Subpolar box include transformations in the northwest Labrador Sea, inferred from the isopycnal fluxes across AR7W (see Figure 1). Similarly, those in the Subtropical box include the Mediterranean Sea.

The dominant pattern of the MOC is the cell of northward thermocline water and AAIW and southward-flowing NADW, centered on model layers 13-14 ($27.70 \leq \gamma^n \leq 27.83$, θ = 6-6.5°C in the Subtropical box). Air-sea buoyancy loss in the subtropical and subpolar gyres (including the Overflow box) converts 10 Sv of water into the density range of Subtropical Mode Water (STMW, $26.2 \leq \gamma^n \leq 27.2$) and 13 Sv into the density range of Subpolar Mode Water (SPMW, $27.35 \leq \gamma^n \leq 27.88$) (similar to Speer and Tziperman, 1992). The strongest diapycnal volume flux is found at light STMW layers in the Subtropical box (an additional parcel is released in one of these layers in Fig.2), where intense cooling and excess evaporation over precipitation is found in the Gulf Stream and Gulf Stream recirculation. At the extreme end of SPMW, deep convection in the Labrador Sea produces Labrador Sea Water (LSW, $27.88 \leq \gamma^n \leq 27.976$), which passes southward in the deep limb of this cell and contributes to upper NADW seen at 11°S. Across the Subpolar and Subtropical boxes, this southward flow remains nearly isopycnal in subsurface layers, with effective diffusivities of order 10^{-5} m^2/s. In the Equatorial box, however, upwelling occurs and effective diffusivities reach 0.5-1 x 10^{-4}m^2/s.

Some fraction of surface water crossing 11°S does not participate in the "mode water" MOC cell, but is instead heated (entering the lightest model layer) in the Equatorial box, then cooled in the subtropical and subpolar gyres (where it passes through STMW to light SPMW densities). A total of 6.4±0.7 Sv enters the Nordic Seas via the Irminger and Norwegian Atlantic Currents, where it is ultimately converted to the overflow water which returns to the North Atlantic (c.f. Mauritzen, 1996).

Of the 3.1±0.9 Sv of AABW flowing north across 11°S, approximately 2 Sv is converted into lower deep water in the Equatorial box, producing a near-bottom effective diffusivity maximum of 6.4±2.5 x $10^{-4} m^2/s$. The remainder, the densest 1 Sv of AABW crossing 11°S, reaches the Subtropical box, is converted to lighter densities, and returns southward across 11°S as lower NADW.

The overflow of Nordic Seas water spans a broad range of densities, including the LSW range. The densest NSOW upwells across isopycnals as it moves southward beneath the main MOC cell, with the most rapid change occurring in the Overflow box. Although we do not resolve the process explicitly, the magnified upwelling in the Overflow box is thought to be due to detrainment as the overflow water passes out of the Denmark Strait and Faroe Bank Channels and into the mouths of the Irminger and Iceland Basins of the North Atlantic in overflow plumes. Less-dense NSOW trajectories plunge sharply downward in the Overflow box, beneath layers in contact with the surface, suggesting entrainment of light overflow water (along with dense SPMW) into the overflow plumes. The convergence of light and dense NSOW trajectories produces a concentration of trajectories in the density range of lower NADW ($27.976 \leq \gamma^n \leq 28.13$). Across 11°S, 11.4±2.4 Sv of lower NADW passes into the South Atlantic - only 1.5±1.2 Sv passes over the Greenland-Iceland-Scotland ridges in this density range. As noted above, 3.9±0.9 Sv of this increase is fed by AABW. We interpret much of the remainder as a consequence of the entrainment/detrainment process within the descending NSOW plumes. Thus, these plumes are a fundamental element of the North Atlantic Ocean's meridional overturning circulation.

Acknowledgements

We would like to thank Amit Tandon and Bernadette Sloyan for their input and assistance. This work was supported by NSF grant OCE-9906657, "Large-scale property fluxes in the North Atlantic."

References

Bacon, S. 1997: Circulation and fluxes in the North Atlantic between Greenland and Ireland. J. Phys. Oceanogr. 27, 1420-1435.

Bersch, M. 1995: On the circulation of the northeastern North Atlantic. Deep Sea Res., Part I 42, 1583-1607.

da Silva, A. M., C. C. Young, and S. Levitus, 1994: Atlas of Surface Marine Data 1994 Volume 1: Algorithms and Procedures. Technical report, National Oceanic and Atmospheric Administration. 51 pp.

Dornblut, I., W. Grabs, and T. de Couet, 1998: Product 1: Freshwater Surface Water Fluxes into the World Oceans, Marginal and Inland Seas. Technical report, Global Runoff Data Centre, Koblenz, Germany.

Girton, J. B., T. B. Sanford, and R. H. Kase, 2001: Synoptic sections of the Denmark Strait Overflow. Geophys. Res. Letters 28, 1619-1622.

Hall, M. M., M. McCartney, and J. A. Whitehead, 1997: Antarctic bottom water flux in the equatorial western Atlantic. J. Phys. Oceanogr. 27, 1903-1926.

Hansen, B., K. M. H. Larsen, S. Osterhus, B. Turrell, and S. Jonsson, 1999: The Atlantic Water Inflow to the Nordic Seas. International WOCE Newsletter 35, 33-35.

Jackett, D. R. and T. J. McDougall, 1997: A neutral density variable for the World's Oceans. J. Phys. Oceanogr. 27, 237-263.

Josey, S. A., E. C. Kent, and P. K. Taylor, 2001: On the Wind Stress Forcing of the Ocean in the SOC and Hellerman and Rosenstein Climatologies. J. Phys. Oceanogr. (submitted).

Lazier, J. R. N. and D.G. Wright, 1993: Annual Velocity Variations in the Labrador Current. J. Phys. Oceanogr. 23, 659-678.

Lumpkin, R. and K. Speer, 2002: Mixing and recirculation in the North Atlantic Ocean. In preparation.

Mauritzen, C., 1996: Production of dense overflow waters feeding the North Atlantic across the Greenland-Scotland Ridge. Deep Sea Res., Part I 43, 769-835.

Mercier, H. and K. G. Speer, 1998: Transport of bottom water in the Romanche Fracture Zone and the Chain Fracture Zone. J. Phys. Oceanogr. 28, 779-790.

Price, J., T. Sanford, C. Mauritzen, and M. Prater, 2001: A Report of XCP and CTD data taken during June, 2001, RRS Discovery cruise 247B, A Process Study of the Faroe Bank Channel Overflow. Res. Rep. April 19, Woods Hole Oceanographic Institution.

Ross, C. K., 1984: Temperature-salinity characteristics of the "overflow" water in Denmark Strait during "OVERFLOW `73". Rapport et Proces-verbaux Reunion Conseil Internationale Exploration de la Mer 185, 111-119.

Saunders, P. M., 1990: Cold outflow from the Faroe Bank Channel. J. Phys. Oceanogr. 20, 29-43.

Schott, F. A., T. N. Lee, and R. Zantopp, 1988: Variability of structure and transport of the Florida Current in the period range of day to seasonal. J. Phys. Oceanogr. 18, 1209-1230.

Speer, K. G. and E. Tziperman, 1992: Rates of water mass formation in the North Atlantic Ocean. J. Phys. Oceanogr. 22, 93-104.

Speer, K. G. 1997: A note on average cross-isopycnal mixing in the North Atlantic ocean. Deep Sea Res. 44, 1981-1990.

Wijffels, S. E., R. W. Schmitt, H. L. Bryden, and A. Stigebrandt, 1992: Transport of Freshwater by the Oceans. J. Phys. Oceanogr. 22, 155-162.

Wunsch, C. 1996: The Ocean Circulation Inverse Problem. New York: Cambridge University Press.

Climatological mean heat transport and its variability in the coupled climate model HadCM3

Michael Vellinga and Helene Banks,
Met Office, Hadley Centre for Climate Prediction and Research, London Road, Bracknell RG12 2SY UK.
michael.vellinga@metoffice.com

1 Introduction

Much research is devoted to obtaining estimates of oceanic heat transport. Both mean ocean heat transport and transport variability are important to climate. Variability in ocean heat and freshwater transport may reflect changes in both oceanic and atmospheric conditions. Due to these coupled dynamics, ocean-atmosphere general circulation models can provide a valuable tool for estimating and understanding variability of ocean transports. Here we use HadCM3, which is the most recent version of the Met Office's Hadley Centre climate model. This is a coupled ocean-atmosphere-sea ice general circulation model. The ocean component has a horizontal resolution of 1.25º x 1.25º, with 20 vertical levels, 10 of which are located in the upper 300 m. It does not require the use of flux adjustment to maintain a stable surface climate (Gordon et al., 2000). Implied meridional transports that can be associated with flux adjustment and which are independent of climate state and thus unphysical are not present in HadCM3. In this article we present aspects of annual mean meridional heat transport in HadCM3. Our aim is to provide quantitative information of the degree of variability in ocean heat transport, as well as some preliminary indications about the processes underpinning the variability. We do not provide a comprehensive analysis here.

During the first 360 years of the control integration of over 1500 years, the ocean and atmosphere transport come into balance (Pardaens et al., 2001). We have used the subsequent 940 years of data. The control integration was run with fixed, pre-industrial CO_2 levels. We will discuss the mean transports in the Atlantic and Indo-Pacific basins in Section 2. In Section 3 we will discuss aspects of variability of the heat transport, and also sketch some of the dominant mechanisms that are associated with the variability in this climate model.

2 Transport

The annual mean total northward heat transport in the Indo-Pacific (Fig. 1a) is directed poleward in both hemispheres. In the tropics the transport is dominated by the overturning component. Heat transport by the gyre component changes from being equatorward in the tropics, to poleward at higher latitudes. Mixing contributes little to the total meridional transport. In HadCM3 meridional transport due to mixing is a combination of isopycnal mixing and the eddy parameterisation scheme of (Visbeck et al., 1997). Observed (Macdonald, 1998) and model heat transports agree well overall, but only marginally so at 48°N. There is strong variability in the annual mean heat transport in large parts of the Indo-Pacific, with peaks in the tropics and subtropics (with a standard deviation of 0.1-0.4 PW). This variability resides largely in the overturning component.

In the Atlantic Ocean (Fig. 1b) the annual mean heat transport is northward, and is dominated by the meridional overturning over most of the basin. Variability is weaker than in the Indo-Pacific, the standard deviation is typically less than 0.1 PW. In various parts of the Atlantic, HadCM3

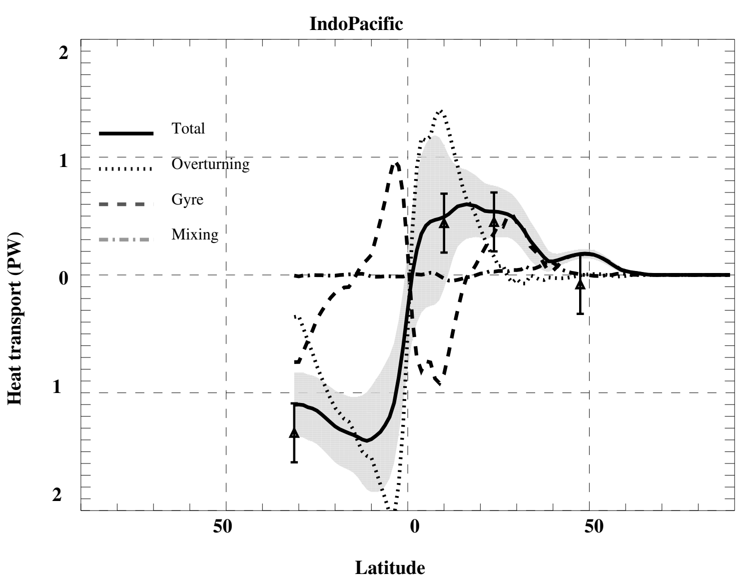

***Figure 1a**:*
Latitudinal profiles of northward heat transport in the combined Indo-Pacific oceans. The mean total transport (solid) has been decomposed into contributions by the zonal mean currents and temperature ('Overturning', dotted); departures from the zonal mean currents and temperature ('Gyre', dashed); mixing due to diffusion of heat ('Mixing', dash-dotted). The grey shading indicates the range of two standard deviations of the total annual mean transport. Observational estimates of heat transport (Macdonald 1998) are given by the black triangles, together with appropriate error bars.

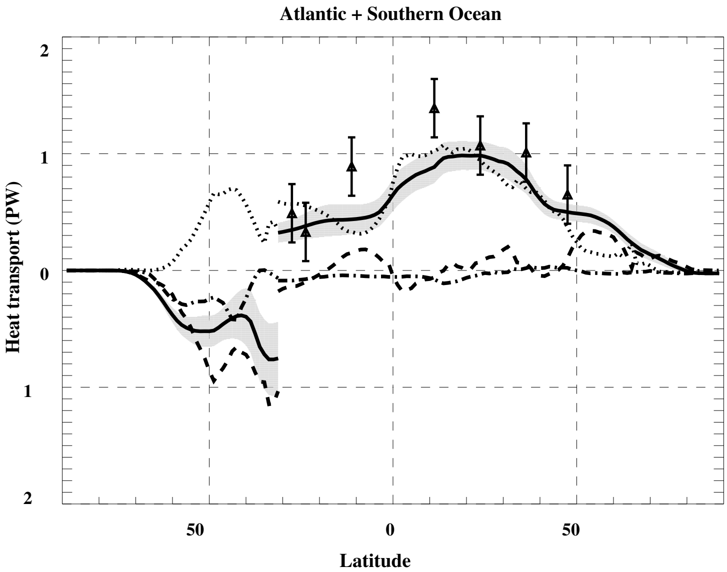

***Figure 1b**:*
As in Figure 1a, but for heat transport in the Atlantic Ocean (north of 30° S) and Southern Ocean (south of 30° S).

of the variability in the total heat transport can be explained by the variability of the local (zonal mean) meridional Ekman transport. Variability of wind stress is thus an important mechanism in forcing heat transport variability, either directly by driving a near-surface Ekman transport, or by the subsequent interior barotropic response.

In the North Pacific variability is comparatively weak. A small (but statistically significant) fraction of the variability in the North Pacific appears to be linked to the NAO.

underestimates the mean meridional heat transport, compared to the observations of Macdonald (1998). In the model, the North Atlantic Deep Water is too warm, and the vertical temperature contrast between the northward and southward flow is too small. This reduces the effectiveness of the heat transport by the overturning (Gordon et al., 2000).

Compared to the other basins the heat transport in the Southern Ocean has a substantial contribution from mixing. The strong variability in the heat transport is largely caused by the advective transport.

3 Variability of heat transport

In the Indo-Pacific south of 40ºN, most of the variability is concentrated in short periods of up to 10 years (Fig. 2a, page 16). Significant amounts of power, exceeding those that may be expected of a pure red-noise process, are present in the spectral range between 3-10 years. ENSO variability in HadCM3 has a spectral peak concentrated in a similar frequency band (Collins et al., 2001). Up to 30% of the variance in the meridional heat transport in the Indo-Pacific is associated with ENSO (Fig. 3a). A large proportion (up to 80 %)

The power spectra of heat transport in the Atlantic Ocean are more red in character than in the Indo-Pacific (i.e. more energy is concentrated in the longer periods than in the shorter periods). This is particularly the case between about 20ºN-60ºN (Fig. 2b, page 16), where significant power is present at timescales of 50-100 years. Most of the variability in the Atlantic heat transport can be explained by the meridional overturning (Fig. 3b). Variability of Ekman transport is less important than in the Indo-Pacific, but still accounts for up to about 50% of the variability in the North Atlantic. Naturally, mean meridional overturning and meridional Ekman transport are correlated, especially on short timescales. South of about 20ºN variability occurs mainly on interannual timescales (Fig. 2b). There, about 20-30% of the variance can be associated with

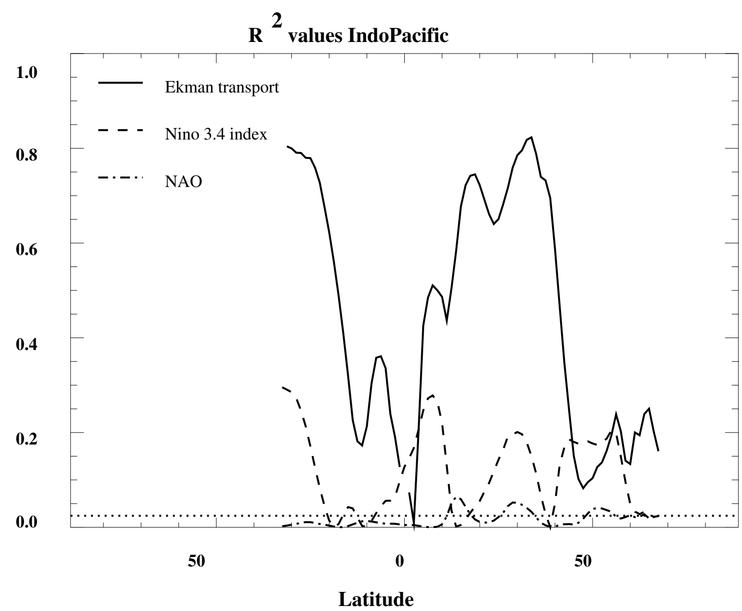

***Figure 3a**:*
Latitudinal distribution of R^2 values (i.e. squared linear correlation) between meridional heat transport in the Indo-Pacific and: Zonal-mean Ekman transport at the same latitude (solid, using 160 years of data), SST anomalies in the Niño-3.4 region (dashed), NAO index (dash-dotted). The 95% significance level is shown by the dotted line.

ENSO (Fig. 3b). Variability of the NAO can explain at most 15% of the variance of heat transport in the subtropical and midlatitude North Atlantic.

In the Southern Ocean variations in zonal windstress/ meridional Ekman transport can explain most of the variability in the meridional heat transport (Fig. 3b). The relationship between ENSO and wind stress anomalies in the Southern Ocean is considerable (not shown).

4 Conclusions

We have presented some quantitative aspects of meridional heat transport in HadCM3, a global ocean-atmosphere GCM that does not use flux adjustments.

In the tropical Indo-Pacific variability occurs mainly on interannual timescales, and has a standard deviation of up to 0.4 PW. This rather large variability suggests that there may be large fluctuations of local ocean heat content and/ or surface heat flux, but we have not checked that in the model as yet. High-resolution observations from XBTs and moorings may provide an important cross-validation (cf. Meinen and McPhaden, 2001). In the model, variability in meridional transport is largely wind-driven. About 20-30% of the variance in the meridional heat transport is connected to ENSO.

In the North Atlantic Ocean additional power is resident in multi-decadal timescales. This is associated with variability of the thermohaline circulation. It is still unclear what physical processes in HadCM3 cause the concentration of energy in these multi-decadal periods beyond the levels of a simple red-noise process.

Acknowledgements

This work was funded by the Department for Environment, Food and Rural Affairs, under the Climate Prediction Programme PECD/7/12/37.

References

Collins M., S.F.B. Tett, and C. Cooper, 2001: The internal climate variability of HadCM3, a version of the Hadley Centre coupled model without flux adjustments, Clim. Dyn., 17, 61-81

Gordon C., C. Cooper, C.A. Senior, H. Banks, J.M. Gregory, T.C. Johns, J.F.B. Mitchell, and R.A. Wood, 2000: The simulation of SST, sea ice extents and ocean heat transports in a version of the Hadley Centre coupled model without flux adjustments, Clim. Dyn., 16, 147-168

Macdonald, A., 1998: The global ocean circulation: a hydrographic estimate and regional analysis, Progr. in Oceanogr., 41, 281-382.

Meinen, C and M.J. McPhaden, 2001: Interannual variability in warm water volume transports in the equatorial Pacific during 1993-99, J. Phys. Oceanogr., 31, 1324-1345.

Pardaens, A., H.T. Banks, J.M. Gregory, and P. Rowntree, 2001: Freshwater transports in HadCM3, subm. Clim. Dyn.

Visbeck, M., J. Marshall, T. Haine, and M. Spall, 1997: On the specification of eddy transfer coefficients in coarse resolution ocean circulation models, J. Phys. Oceanogr., 27, 381-402.

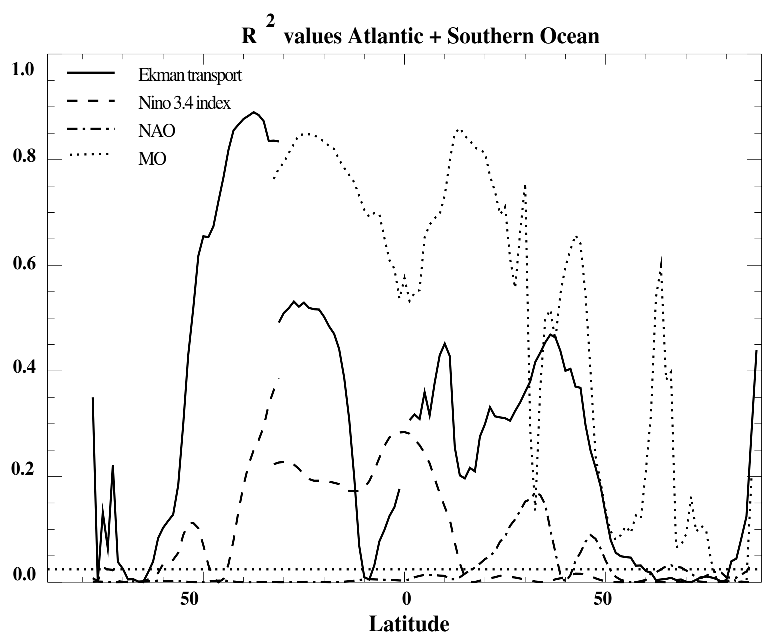

Figure 3b:
As for Figure 3a, but for the Atlantic and Southern Ocean. The dotted curve shows the R^2 values of heat transport and maximum meridional overturning at the same latitude.

Freshwater transports in the Hadley Centre coupled climate model (HadCM3)

Anne Pardaens, Helene Banks, Jonathan Gregory, Peter Rowntree
Met Office, Hadley Centre for Climate Prediction and Research, Bracknell, UK
anne.pardaens@metoffice.com

The hydrological cycle can influence climate through a great variety of processes and it is therefore important that it is well represented in climate models. Studies of the present day hydrological cycle and model validation are hampered by availability of observations relevant to the global hydrological cycle. The self-consistent data available from global coupled model simulations, however, can be used to understand the available observations in the context of a global system. We have looked at large scale aspects of the global freshwater budget in the Hadley Centre coupled climate model (HadCM3) simulation of over 1000 years, concentrating on the Atlantic Ocean where the freshwater budget is likely to be particularly important for the thermohaline circulation (THC). A more complete description of this work can be found in Pardaens et al. (2002).

The HadCM3 model and data used for validation

The HadCM3 atmosphere model has a resolution of 3.75° longitude by 2.5° latitude and 19 vertical levels. The ocean model is based on the Cox (1984) model and has a resolution of 1.25° by 1.25° and 20 vertical levels. The ocean model was initialised with temperatures and salinities from Levitus and Boyer (1994) and Levitus et al. (1994), and allowed to evolve from rest. Further details of the model can be found in Gordon et al. (2000). The HadCM3 control model (with pre-industrial atmospheric gas concentrations) has run for over 1000 years without the need for flux adjustment to maintain a stable climate.

To validate the HadCM3 freshwater budget we have used a precipitation climatology from CMAP/O data (Xie and Arkin, 1997), evaporation calculated from the latent heat field in the SOC ship-based climatology (Josey et al., 1999) and the river runoff climatology of Baumgartner and Reichel (1975). Freshwater transport estimates derived from ocean section measurements have also been used. There are considerable uncertainties in observational data relevant to freshwater budgets over the ocean (Wijffels, 2001). We have chosen to use particular surface flux climatologies on the basis of their likely quality, but the global freshwater flux from these climatologies is not constrained to be in global balance. Enforcing a global balance may, however, degrade the available data (as discussed by (Josey et al., 1999) for heat fluxes). The variety of data types we have used for comparison with the model freshwater budget (surface fluxes, ocean sections, salinity climatology) and model sensitivity tests allow a more robust validation than is possible from more limited data sources.

The HadCM3 global freshwater budget

The HadCM3 global ocean zonal-mean meridional freshwater transports adjust in the first 400 years of the simulation to come into near balance with the atmospheric freshwater transports. This adjustment is achieved by increasing oceanic freshwater transport from the Southern Ocean to more northern latitudes (Fig. 1). A difference between the actual and implied ocean freshwater transport divergence from an ocean volume enclosed by two latitudes will lead to a salinity drift.

The comparison of observation derived estimates of the export of freshwater from the Southern Ocean (Sloyan and Rintoul, 2001; Wijffels, 2001) with model values suggests that, when balanced with the surface fluxes, the model export (and therefore surface freshwater input in this region) is too high. Comparison of the surface freshwater flux with observations (Fig. 2, see page 15) also suggests that generally there is too much evaporation at low to subtropical latitudes. We have found that the distribution of ocean salinity moves to more extreme salinities as the model comes into freshwater balance indicating either deficient mixing processes, or that the surface fluxes are too extreme. In total, our validation has led us to conclude that the model hydrological cycle is likely to be excessive.

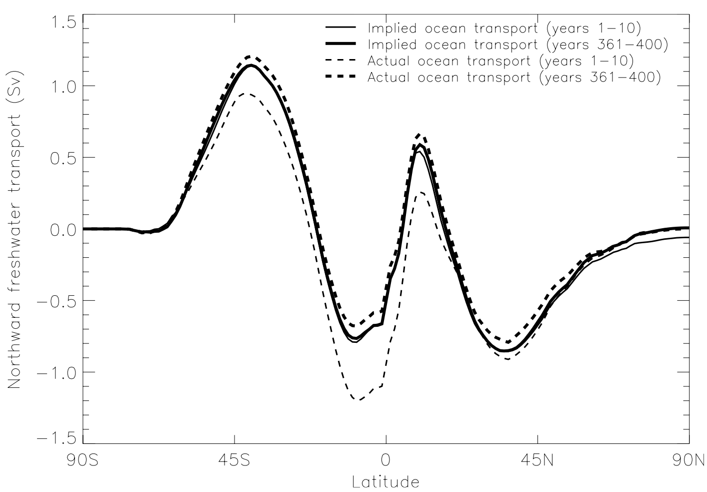

Figure 1:
Global actual and implied (required to balance the surface fluxes) oceanic meridional freshwater transports in HadCM3 for years 1-10 and 361-400. Units are Sv, equivalent to 10^9 kg s^{-1} of surface flux input.

The Atlantic freshwater budget

The Atlantic Ocean is particularly important for the THC, and we have looked at the model freshwater budget in this region in more detail. Increases in northern (approximately 24-66° N) Atlantic volume weighted salinity and temperature are evident over the first 200 years, and similar tropical-subtropical Atlantic drifts take approximately 400 years to stabilise. The increase in northward freshwater transport from the Southern Ocean over the first 400 years of the model simulation increases the freshwater transport into the Atlantic Ocean. This brings it to near balance with the implied transport from the surface fluxes (Fig. 3) and so reduces the Atlantic salinity drifts.

Validation against data suggests that the dominant model freshwater budget error leading to the salinity drifts in the tropical-subtropical Atlantic region is excessive evaporation, and that the dominant error in the northern Atlantic region is a lack of ocean freshwater transport convergence. Model sensitivity tests, which are not discussed here, support this conclusion and also show that the northern Atlantic salinity drift is due to the transport of overly saline water from the lower Atlantic latitudes. The low latitude Atlantic salinity errors, due to the excessive evaporation, advect northwards, sink to depth with the North Atlantic Deep Water and then travel southwards to exit the Atlantic at 30°S, changing the zonal mean temperature and salinity properties over a timescale of approximately 400 years (Fig. 4, page 15).

Rahmstorf (1996) proposed that the equilibrium THC stability is dependent on the component of surface freshwater flux input to the Atlantic basin (to 30°S) that is not removed by the gyre circulation. Rahmstorf (1996) also proposed that the present day overturning circulation exports freshwater from the Atlantic basin, and that this indicates that the equilibrium THC is purely thermally driven. In HadCM3, the overturning circulation initially exports freshwater from the Atlantic, but as the model comes into freshwater balance it imports freshwater. Comparison with the conceptual model of (Rahmstorf, 1996) would suggest that the equilibrium model THC is therefore driven by both thermal and haline components. This may have implications for the stability of the model THC.

Summary

The HadCM3 model appears to have an overly strong hydrological cycle. The ocean transports of freshwater adjust over a period of about 400 years to transport more freshwater from the Southern Ocean into the Atlantic where there is too much evaporation. The overturning circulation component achieves most of this increase by changing from an exporter of freshwater from the Atlantic to an importer of freshwater, in contrast to the situation for the present day THC suggested by (Rahmstorf, 1996). This may have implications for the stability of the model THC.

Acknowledgements

This work was funded by the Department of the Environment, Food and Rural Affairs Climate Prediction Program and the Public Meteorological Service Research Program.

References

Bacon, S., 1997: Circulation and fluxes in the North Atlantic between Greenland and Ireland. J. Phys. Oceanog., 27, 1420-1435.

Baumgartner, A., and E. Reichel, 1975: The world water balance, Elsevier.

Cox, M.D., 1984: A primitive equation, three dimensional model of the ocean. Ocean Group Technical Report 1, GFDL Princeton.

Friedrichs, M. and M. Hall, 1993: Deep circulation in the tropical North Atlantic. J. Marine Res., 51, 697-736.

Gordon, C., C. Cooper, C.A. Senior, H. Banks, J.M. Gregory, T.C. Johns, J.F.B. Mitchell, and R.A. Wood, 2000: The simulation of SST, sea ice extents and ocean heat transports in a version of the Hadley Centre coupled model without flux adjustments. Clim. Dyn., 16, 147-168.

Hall, M.M. and H.L. Bryden, 1982: Direct estimates and mechanisms of ocean heat transport. Deep-Sea Res., 29, 339-359.

Holfort, J. and G. Siedler, 2001: The meridional oceanic transports of heat and nutrients in the South Atlantic. J. Phys. Oceanog., 31, 5-29.

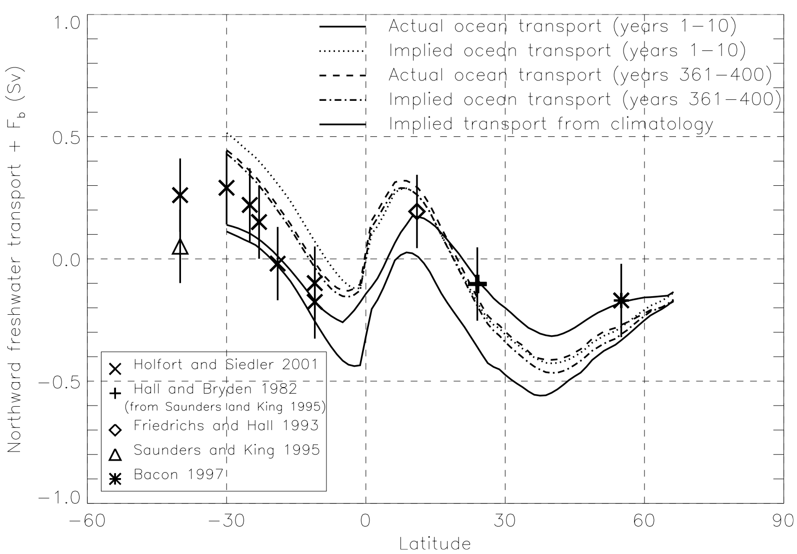

Figure 3:
HadCM3 Atlantic actual and implied northward freshwater meridional transports (in Sv) relative to freshwater transport F_b through Bering Strait. Implied transport from climatological surface fluxes is also shown and symbols show ocean section freshwater transport estimates (derived from information given in papers quoted, error bars after Wijffels (2001)).

Josey, S., E. Kent and P. Taylor, 1999: New insights into the ocean heat budget closure problem from analysis of the SOC air-sea flux climatology. J. Climate, 12, 2856-2880.
Levitus, S. and T.P. Boyer, 1994: World ocean atlas 1994, volume 4: Temperature. NOAA Atlas NESDIS 4, U.S. Government Printing Office, Washington, D.C., 117pp.
Levitus, S., R. Burgett and T.P. Boyer, 1994: World ocean atlas 1994, volume 3: Salinity. NOAA Atlas NESDIS 3, U.S. Government Printing Office, Washington, D.C., 99pp.
Pardaens, A.K., Banks H.T., Gregory J.M. and P.R. Rowntree, 2002: Clim. Dyn., submitted.
Rahmstorf, S., 1996: On the freshwater forcing and transport of the Atlantic thermohaline circulation. Clim. Dyn., 12, 799-811.
Saunders, P., and B. King, 1995: Oceanic fluxes on the WOCE A11 section. J. Phys. Oceanog., 25, 1942-1958.
Sloyan, B. and S. Rintoul, 2001: The Southern Ocean limb of the global deep overturning circulation. J. Phys. Oceanog., 31, 143-173.
Wijffels, S., 2001: Ocean transport of fresh water. Ocean circulation and climate, pp.475-488, Academic Press.
Xie, P., P.A. Arkin, 1997: Global precipitation: A 17-year monthly analysis based on gauge observations, satellite estimates and numerical model outputs. Bulletin of the American Meteorological Society, 78(11), 2539-2558.

Oceanic state during 1993-1999 determined by 4-D VAR data assimilation

J. Staneva, M. Wenzel and J. Schröter
Alfred Wegener Institute for Polar and Marine Research, Bremerhaven, Germany
jstaneva@awi-bremerhaven.de

This paper presents progress in a recent study of assimilating data into a global ocean general circulation model (OGCM). The Hamburg LSG (Large Scale Geostrophic) model is used to study the state of the ocean. It is a coarse resolution OGCM (3.5°x 3.5° in the horizontal and 11 vertical levels) originally designed for climate studies. The implicit formulation in time of the LSG allows for a time step of one month. The initial state is taken from its optimized climatological annual cycle obtained by Wenzel et al. (2001), who assimilated monthly temperature and salinity from Levitus, sea surface height as well as the transport of mass, heat and freshwater.

For our purposes the model is forced subsequently with monthly data from the NCEP reanalysis project for 1950-1999. We will refer to this as a reference run (REF). The oceanic state determined by REF will be compared to the results from an optimizated solution (OPT), in which the model is fitted to seven years (1993-1999) of TOPEX/POSEIDON (T/P) data using the adjoint method. The adjoint assimilation technique is the same as in Wenzel et al. (2001). The T/P data are taken relative to the EGM96 geoid model.

As control parameters for the optimisation, we use the model initial temperature and salinity state as well as the mean annual cycle of the wind stress, air temperature and freshwater flux, while the additional temporal variability of the forcing is taken from the NCEP reanalysis from 1992 to 1999. The first-guess initial model state and forcing fields in OPT are taken from the oceanic state from the reference run in January 1992. Additionally we utilize the same data sets as in Wenzel et al. (2001), but with reduced weights.

Model results and comparisons with the data

First we compare the simulated sea surface height (SSH) from the REF and OPT experiment respectively with the T/P data. The seven-year (1993-1999) mean patterns of the RMS deviations of SSH of REF solution (Fig. 1a) and OPT solution (Fig. 1b) from the T/P data revealed a considerable improvement of the assimilation with respect to the diagnostic run. The differences between the altimetry data and model simulations are largest in the equatorial Pacific and Indian oceans, but are significantly reduced in OPT (6 cm vs. 2 cm, respectively). The strong deviations in north Atlantic indicate that the model transports are too weak in REF, and are improved by the assimilation run OPT (see also Fig. 3a,).

The largest deviations in OPT are observed in the regions of strong currents, but are reduced in comparison with those in REF. The seven-year area mean RMS deviations of SSH between the model and the data is 2.67 cm (REF vs. T/P) and 1.23 cm (OPT vs. T/P). The correlations between both model solutions and altimetry data are 0.47 and 0.89, respectively. The area mean SSH variability (see Fig. 2) in the constrained solution (dashed line) from 1993 to 1999 is closer to that of the T/P data (full line). Some deviations from the T/P data are observed after 1998, though much stronger in REF (dotted line).

The global heat transport is constrained by the mean of the estimates of Talley (1984) and Hsiung (1985), hereafter referred to as TH, while for the Atlantic transport we use the data given by Schlitzer (1993) (S93). The Atlantic heat transport (Fig. 3a) fits well to the S93 estimates in OPT

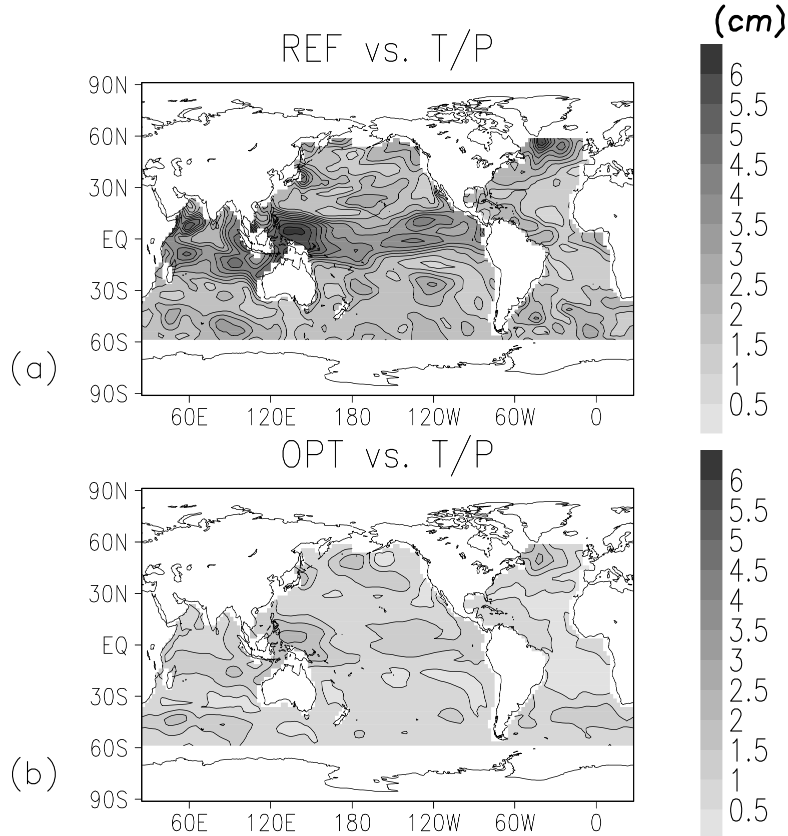

Figure 1.
Temporal mean (1993-1999) RMS deviations of sea surface height [cm] between REF and T/P data (a); between OPT and T/P data (b);

(dashed line) within the errors (grey shading), while for the REF solution it is underestimated. In the Pacific (Fig. 3b) the heat transport is constrained with individual section estimates of Macdonald (1995) (M95) and Sloyan (1997). In both runs the Pacific heat transport is close to the estimates, but the locations of the minimum (from 2.5°S in REF to 12.5°S in OPT) and the maximum (12.5°N in REF vs. 22.5°N in OPT) are shifted by the optimization to fit better with the data.

The temperature and salinity of the OPT solution are constrained using Levitus monthly mean climatological fields (Levitus, 1994). Below we will compare the model simulations with this climatology, as well as with the independent data set taken from WOCE hydrography. Similar comparisons have been done previously by (Stammer et al., 2001).

On Fig. 4 (page 16) we show a meridional temperature section across the central Pacific located at the WOCE section P14 (179°E) and averaged in the time from June to August, 1993 from the assimilation experiment OPT and from the WOCE data. The WOCE data are interpolated to the model grid, therefore all small scale structures related to the eddies in the WOCE hydrography, which are observed in Stammer et al. (2001), are eliminated.

The large-scale structures are simulated by OPT with visually good agreement (see Fig. 4). The difference fields between assimilation results and WOCE data, as well as between OPT and the Levitus data (LEV) are displayed on Fig. 5a and Fig. 5b, (page 17) respectively. The differences are most pronounced in the upper 500 m. In the tropical and equatorial Pacific sub-surface temperature in OPT exceeds that of the data, indicating the deficiencies in the model due to its coarse horizontal resolution.

Below 300 m, the assimilation produces temperatures lower than the climatology (Fig. 5b). This negative deficit is slightly reduced when compared to the WOCE hydrography (Fig. 5a). It is clearly seen from Fig. 5 that the temperature of the assimilation experiment compares better to the independent temperature of the WOCE section than to the Levitus climatology, indicating that the model stratification tends to be closer to the real hydrographic data than to climatology.

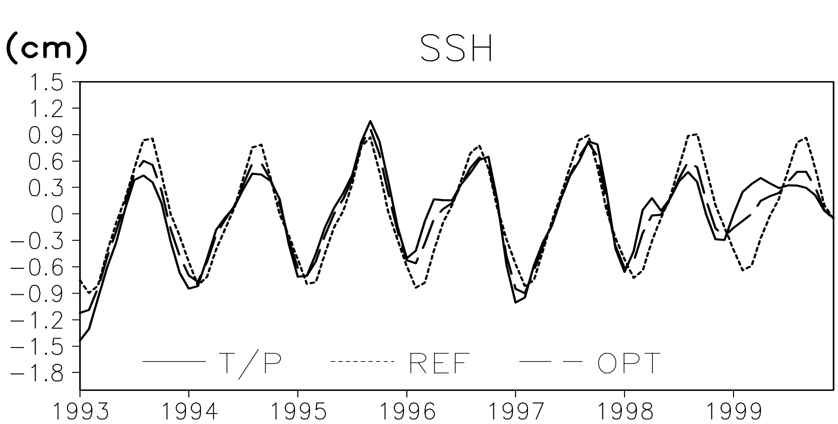

Figure 2.
Area mean sea surface height [cm] as a function of time (c): full line-T/P data, dotted line-REF data; dashed line-–OPT data.

A further comparison between the solutions of the constrained model OPT, the WOCE hydrology and the Levitus climatology is shown in Fig. 6 (page 17) for the zonal section across the North Atlantic (A05-24.5°N). The optimized model temperatures in the upper layers are lower than that of the WOCE data set (Fig. 6a) and much lower than the Levitus climatology (the temperature difference between OPT and Levitus temperature is about 1.5° in the western Atlantic, see Fig. 6b).

However, in the deeper layers, the temperature from OPT is slightly higher that that of the Levitus climatology (in the layer between 2000 and 3000 m) and WOCE hydrography (in the layer between 1000 and 2000 m, west Atlantic), but stays within the prescribed error estimates. These comparisons clearly demonstrate the improvement achieved by constraining the model to the data.

Conclusions

In this study we estimated an optimal ocean state for the seven year period 1993-1999 by 4D-VAR data assimilation. It is clearly seen that the spatial distribution and the temporal evolution of the sea surface height anomaly from the constrained model OPT is closer to altimetry than the unconstrained reference run REF. The correlation of the sea level height between the model and T/P data is significantly improved in OPT. The temporal mean Atlantic and Pacific heat transport fit well to the data. Furthermore it should be emphasised that the temperature fields in OPT are closer to the independent WOCE hydrography than to the Levitus climatology used in the constraints. Giving most weight to the constraints on sea surface height improves the density of the model to a structure more realistic than climatology.

Acknowledgements

This work was supported by the SEAL Project.

References

Hsiung, J., 1985: Estimates of global meridional heat transport. J. Phys. Oceanogr., 15, 1405-1413.

Levitus, S., R. Burgett and T. Boyer, 1994: World Ocean Atlas 1994, vol. 3, Salinity and vol. 4, Temperature, NOAA Atlas NESDIS 3 & 4, U.S. Dept. of Comm., Washington, D.C.

Macdonald A.M., 1995: Oceanic fluxes of mass, heat and freshwater: a global estimate and perspective. Ph.D. Thesis, MIT, Cambridge 02139, 326pp.

Schlitzer, R., 1993: Determining of Mean Large-scale circulation of the Atlantic with the adjoint method. J. Phys. Oceanogr., 2, 1935-1952.

Stammer, D, S. Wunsch, R. Giering, C. Eckert, P. Heimbach, J. Marotzke, A. Adcroft, C. Hill and J. Marshal, 2001: The global ocean circulation during 1992-1997, estimated from ocean observations and a general circulation model, J. Geophys. Res., (submitted).

Talley, L.D., 1984: Meridional heat transport in the Pacific Ocean. J. Phys. Oceanogr., 14, 231-241

Wenzel, M, J. Schröter and D. Olbers, 2001: The annual cycle of the global ocean circulation as determined by 4D VAR data assimilation. Progr. in Oceanogr., 48, 73-119.

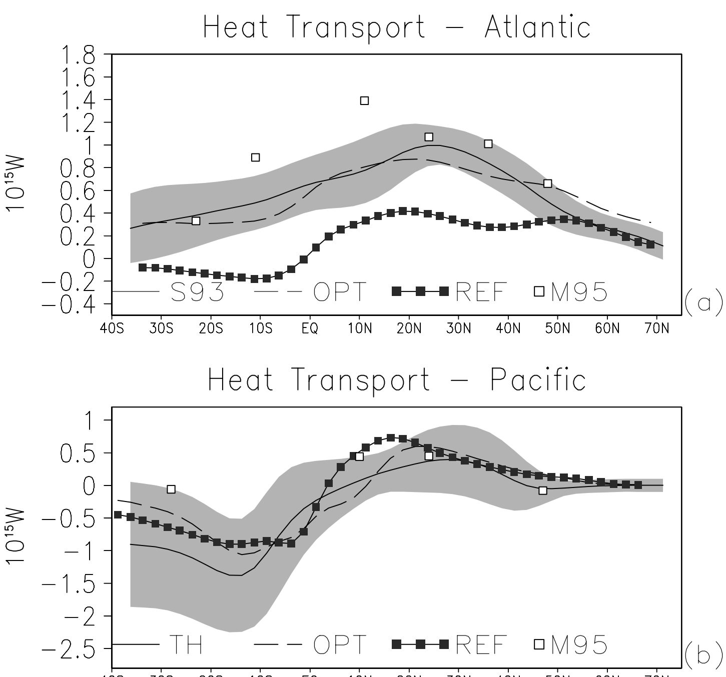

Staneva, et al., *Figure 3*.
Temporal mean meridional heat transport (10^{15} W) for the Atlantic (a) and Pacific (b) oceans. Line with full squares-REF; dashed line-OPT, full line-data compiled from various estimates, e.g. Schlitzer (1993, S93) for Atlantic and (Talley 1984) and (Hsiung 1985, TH) for Pacific with error bars (grey shading). Empty squared symbols correspond to the estimates of Macdonald (1995, M95).

Subtropical Atlantic carbon transport

A. M. Macdonald, M. O'Neil Baringer[1], K. Lee[1], D. Wallace[2] and R. Wanninkhof[1]
CIMAS, RSMAS, University of Miami, Miami, FL, USA.
[1] NOAA/Atlantic Oceanographic and Meteorological Laboratory, Miami, FL, USA.
[2] University of Kiel, Kiel, Germany.
amacdonald@whoi.edu

Over the last decade fossil fuel burning has released approximately 6.2 PgC (1 PgC = 1 GtC = 10^{15} g of carbon) into the atmosphere (Battle et al., 2000). The amount of carbon in the atmosphere, however, has increased at a rate of only 2.8 PgC yr^{-1} (1 PgC yr^{-1} = 1GtCyr^{-1} = 2642 kmolCs^{-1}). The increased partial pressure of atmospheric CO_2 has caused, through air-sea exchange, the amount of carbon stored in the ocean to increase by 2.0±0.6 PgC yr^{-1} (Battle et al., 2000; Schimel et al., 1996; Siegenthaler and Sarmiento, 1993). These estimates strongly suggest that the ocean and ocean circulation are significant players in the global carbon cycle, which determines the rate of the atmospheric increase in CO_2. Nevertheless, just where the oceanic uptake and release of carbon (and in particular the anthropogenic component of carbon (C_{ANTH}), is occurring) and how circulation and mixing affect the oceanic sources and sinks is not well understood. Until recently direct oceanic observations have been sparse and numerical models (which have been extremely good at producing similar net ocean CO_2 storage estimates) have failed as yet to produce a consensus on where the uptake and storage of anthropogenic carbon is occurring (Wallace, 2001). This study seeks to better understand one piece of this puzzle, the transport of carbon within the North Atlantic. In this note we focus on the carbon transport across 24.5°N.

In the summer of 1992, and again in the winter of 1998, hydrographic cruises across 24.5°N latitude in the Atlantic obtained detailed measurements of the oceanic carbon field. These datasets are the result of an increased effort to directly measure carbon dioxide concentrations in seawater during WOCE, the Ocean-Atmosphere Carbon Exchange Studies (OACES) and the U.S. Joint Global Ocean Flux Study (JGOFS) programs. Rosón et al. (2001) presented inorganic carbon and anthropogenic carbon transport estimates based on data from the 1992 occupation of the 24.5°N transect. We compare their data and results to those from the 1998 occupation of the same section.

Using both data sets and simple, mass balancing, inverse box models with Hellerman and Rosenstein (1983) winds, the meridional transport of total inorganic carbon across this latitude is estimated to be -0.74±0.91 PgC yr^{-1} and -1.32±0.99 PgC yr^{-1} southward in 1998 and 1992, respectively. Previous estimates are shown in Table 1. The earliest (Brewer et al., 1989) was based on carbon measurements taken at just nine stations from the late autumn of 1988, combined with the transport results of the full hydrographic transect made in 1981 (Hall and Bryden, 1982). The Rosón et al. (2001) estimates are based on the 1992 dataset using a more classical water mass analysis method for determining the absolute velocity field.

It is generally thought that the tropical Atlantic outgasses carbon, while the subpolar Atlantic absorbs it, leading to large regional divergences. The new estimates presented here are lower than the meridional carbon transport suggested by the Rosón et al. (2001) study and thus imply a smaller divergence (Figure 1). The uncertainty in the carbon transports themselves are a hindrance to determining the 'true' picture. In particular it should be noted that our model was unable to produce the small uncertainty O(0.08 PgC yr^{-1}) (equivalent to a mass transport uncertainty O(0.09 x 10^9Kg s^{-1})) suggested by previous studies. Seasonal effects are also important as colder waters can hold greater concentrations of carbon than warmer waters. Circulation differences are largely responsible as the total inorganic carbon transports are strongly correlated with the patterns and magnitude of mass transport (Macdonald et al., 2002).

Fields of anthropogenic carbon (C_{ANTH}), which cannot be measured, have been estimated using the method of Gruber et al. (1996). Objectively mapping and differencing these fields reveals an increase in C_{ANTH} concentrations in the upper water column over the 6 year period (Figure 2, page 18). Differences at individual grid points are only significant in the region of the deep western boundary current and across the basin at about 1000 m. The magnitude of these changes are of the order of 10μmol kg^{-1}. Horizontal averaging across the basin shows significant increases greater that 5μmol kg^{-1} down to 2000 m. The depth to which the differences are seen is somewhat surprising, but it should be emphasized that the only deep modifications which are locally significant appear in the relatively recently ventilated deep western boundary current waters. If the surface mixed layer total inorganic carbon kept pace with the atmospheric increase we would expect an approximately 6μmol kg^{-1} increase over this time period within the surface layer (Lee et al., 2000). We find that 1) the observed surface increases are of the expected order of magnitude due to anthropogenic changes and 2) a longer record would improve our ability to observe significant changes in C_{ANTH}.

The associated meridional transport of C_{ANTH} across the two transects based on these fields is northward at 0.20±0.08 PgC yr^{-1} and 0.17±0.06 PgC yr^{-1} for the 1998 and 1992 sections, respectively (Table 1). These estimates are consistent with each other, as well as with previous estimates. Concentrations of C_{ANTH} vary a great deal within the water column (1998 mean C_{ANTH} = 13±15μmol kg^{-1}). They are surface intensified

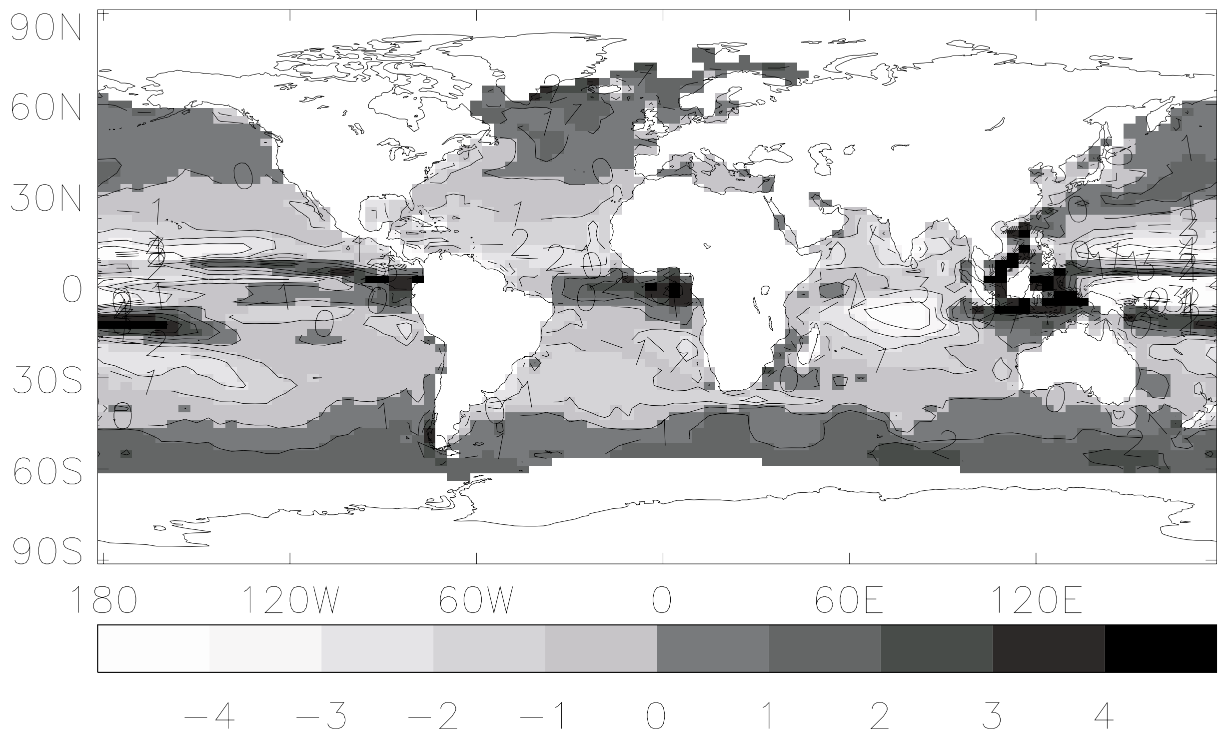

Pardeans et al., ***Figure 2****:*
HadCM3 (years 361-400) precipitation minus evaporation error from climatology (units mm day^{-1}).

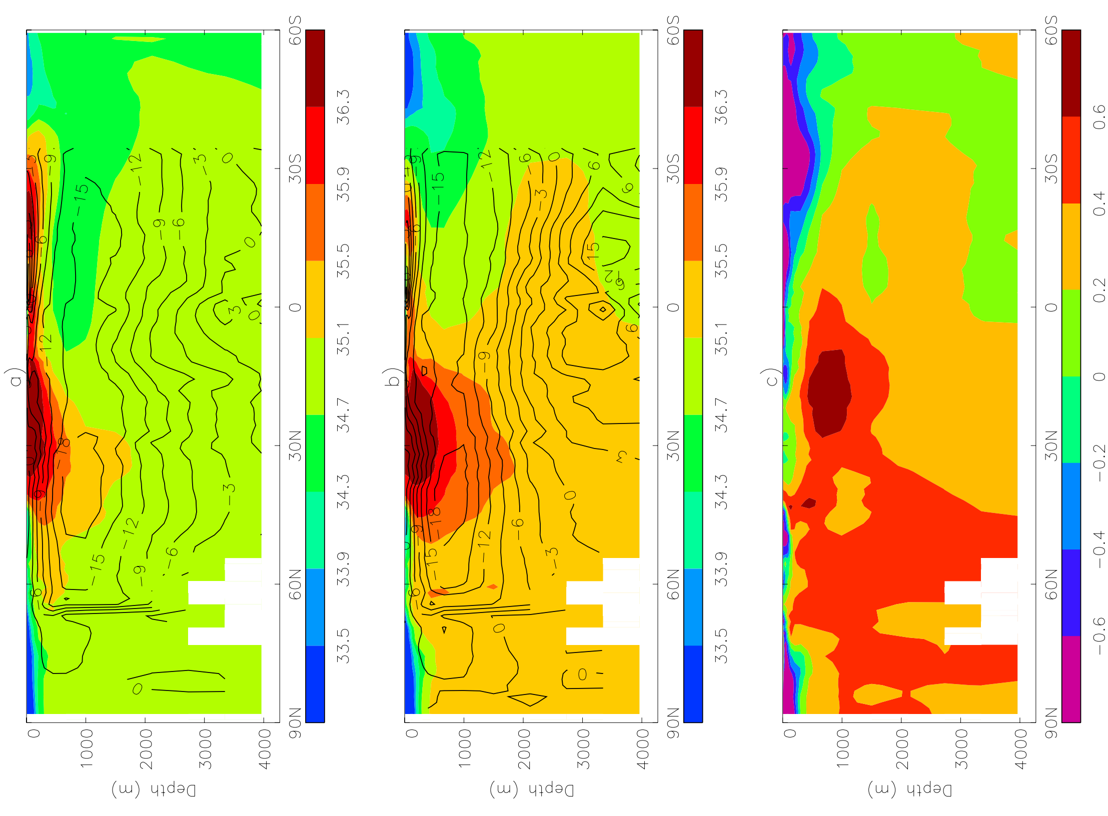

Pardaens, et. al., ***Figure 4****:*
HadCM3 Arctic, Atlantic and Atlantic Southern Ocean a) zonal mean salinity (units psu) overlaid with overturning streamfunction contours for a1-10 b) as a) for years 361-400 c) zonal mean salinity error (units psu) from(Levitus et al., 1994) climatology for model years 361-400.

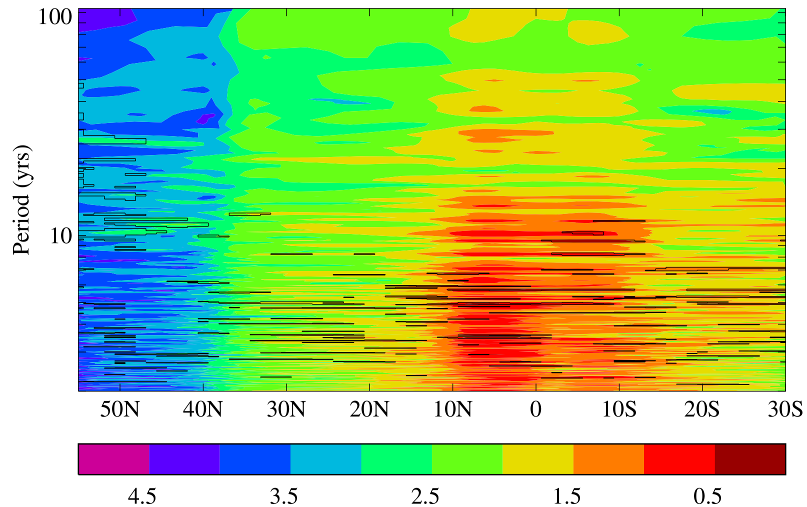

***Vellinga & Banks Figure 2a**:*
Power spectral density as a function of period (vertical axis, in years) and latitude (horizontal axis), for the Indo-Pacific. Shown in grey is the 10-log of power. The contour indicates power exceeding the 95[th] percentile of an AR(1) (red-noise) process.

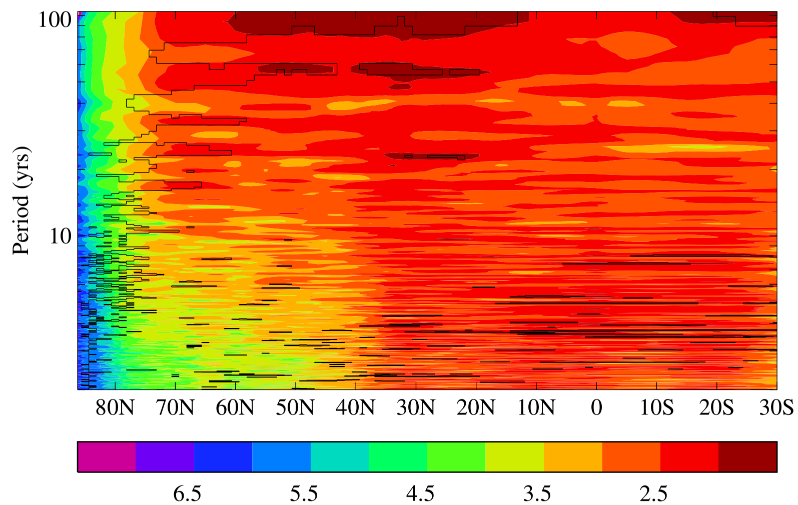

***Vellinga & Banks Figure 2b**:*
As for Figure 2a, but for the Atlantic Ocean.

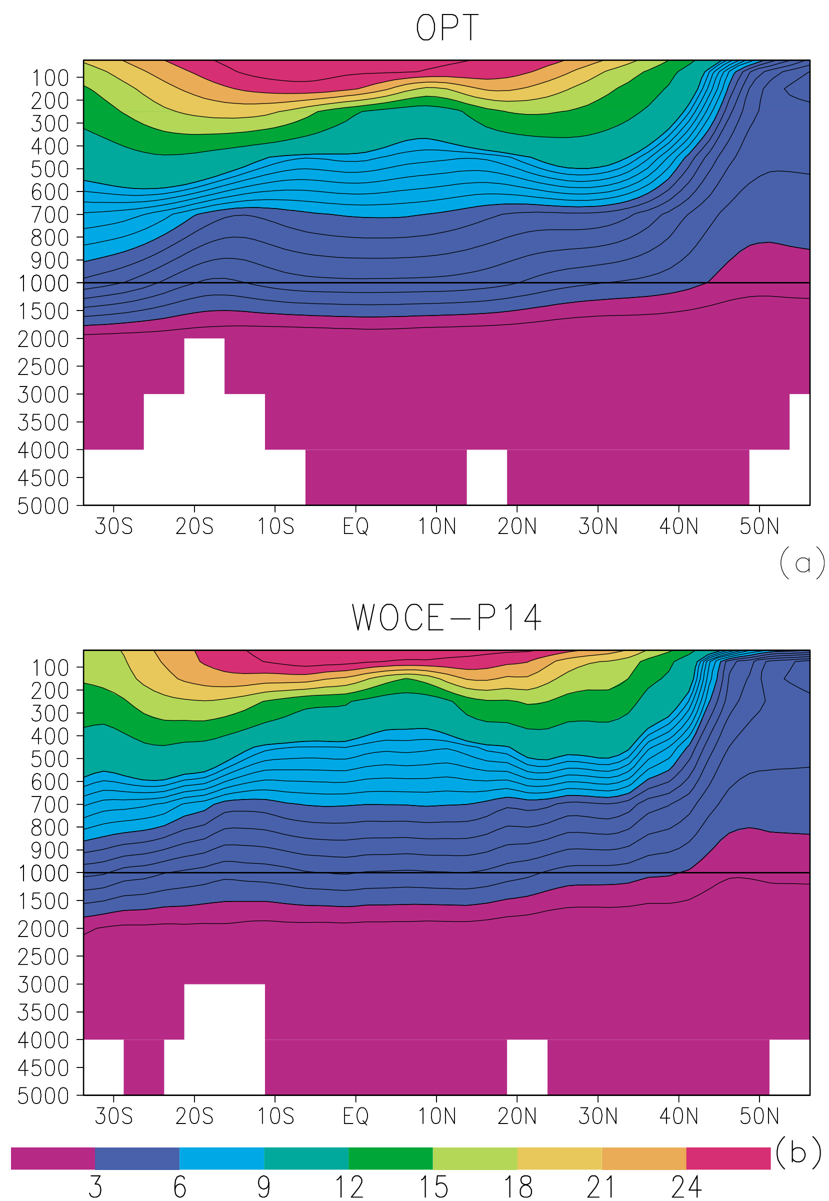

Staneva, et al., *Figure 4.*
A comparison of depth-latitude section of temperature (° C) taken at 179°E across Pacific and time averaged between June 1993 ad August 1993 for: (a) OPT simulations; (b) WOCE data.

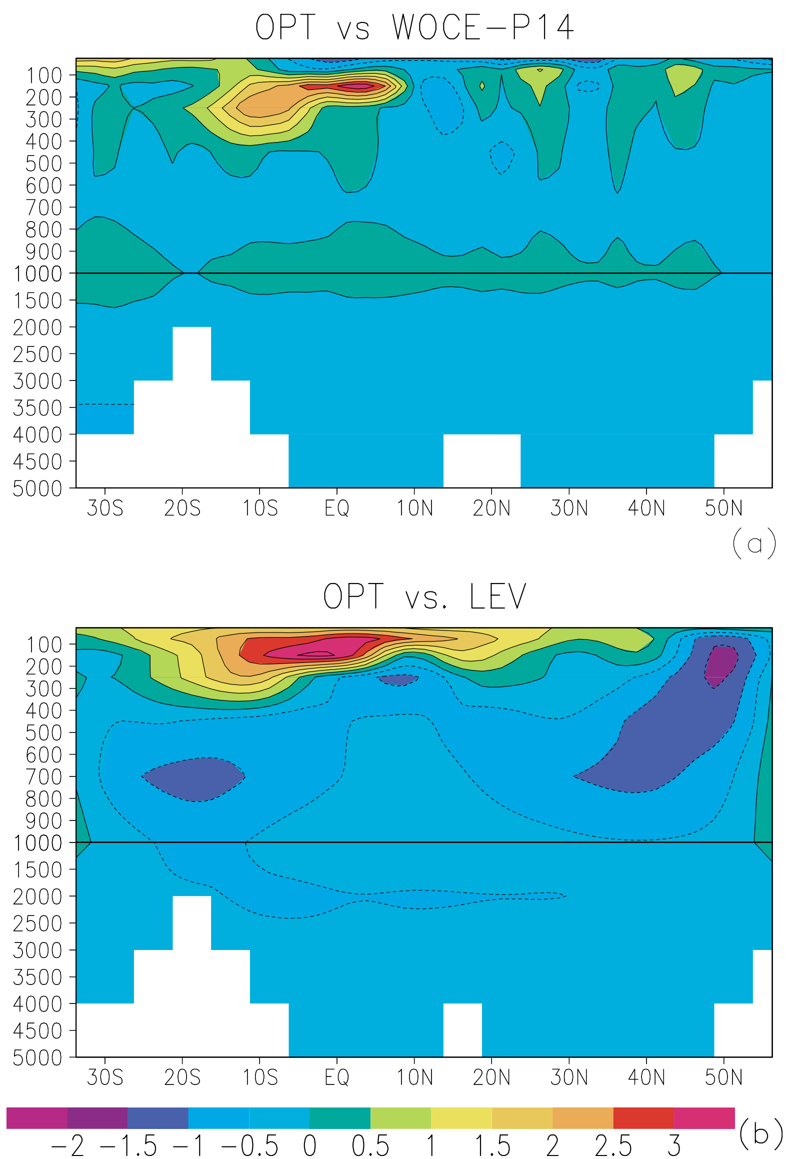

Staneva, et al., *Figure 5.*
Temperature difference at meridional section 179°E across Pacific averaged from June to August, 1993 between (a) OPT vs. WOCE data and (b) OPT vs. Levitus (1994) data.

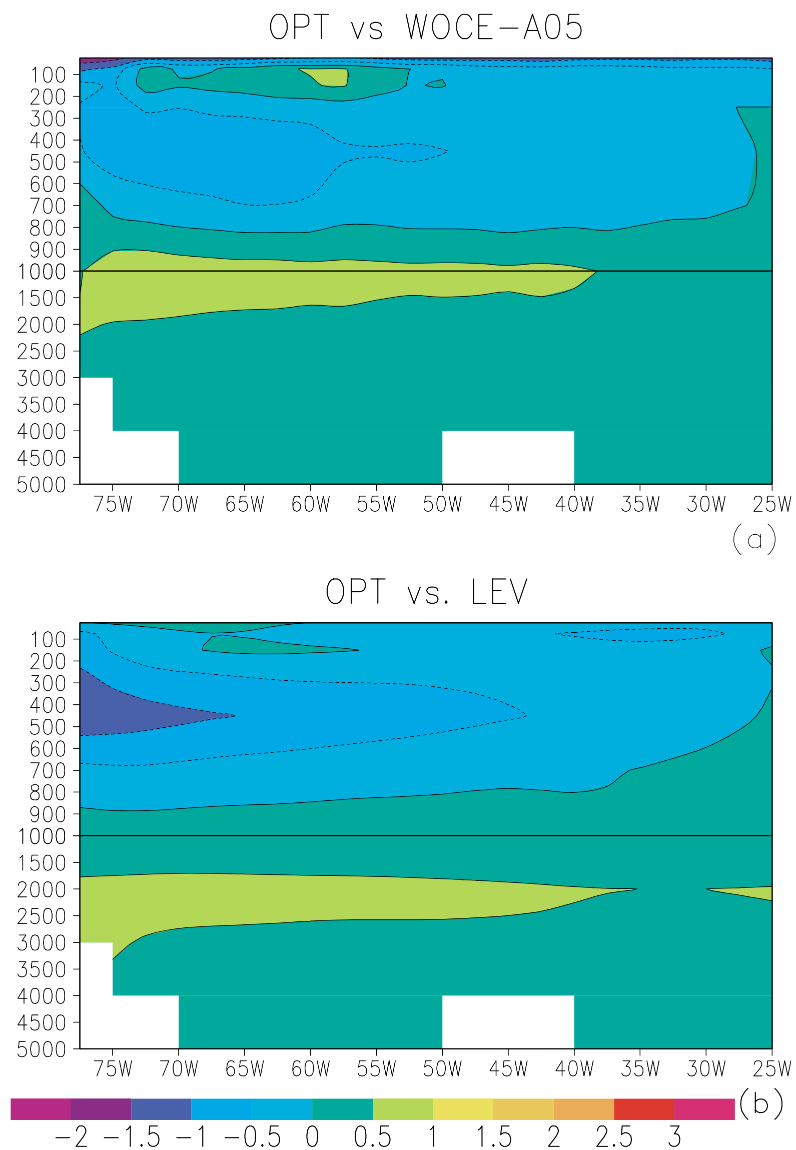

Staneva, et al., *Figure 6*.
Temperature difference along 23.5°N across Atlantic between (a) OPT estimates and WOCE data; (b) between OPT estimates and Levitus (1994) hydrology.

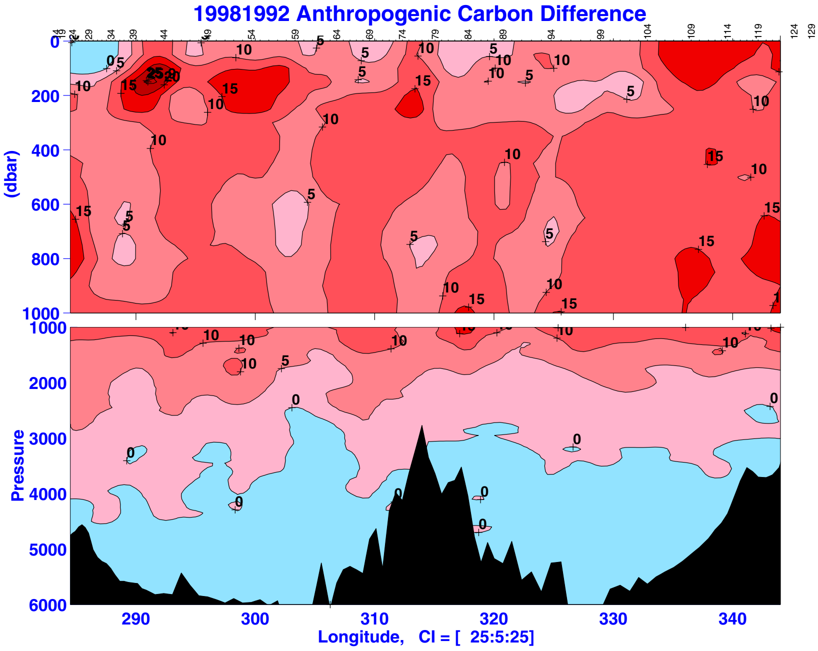

Macdonald, et. al., Figure 2:
The 1992 field of anthropogenic carbon subtracted from the 1998 field.

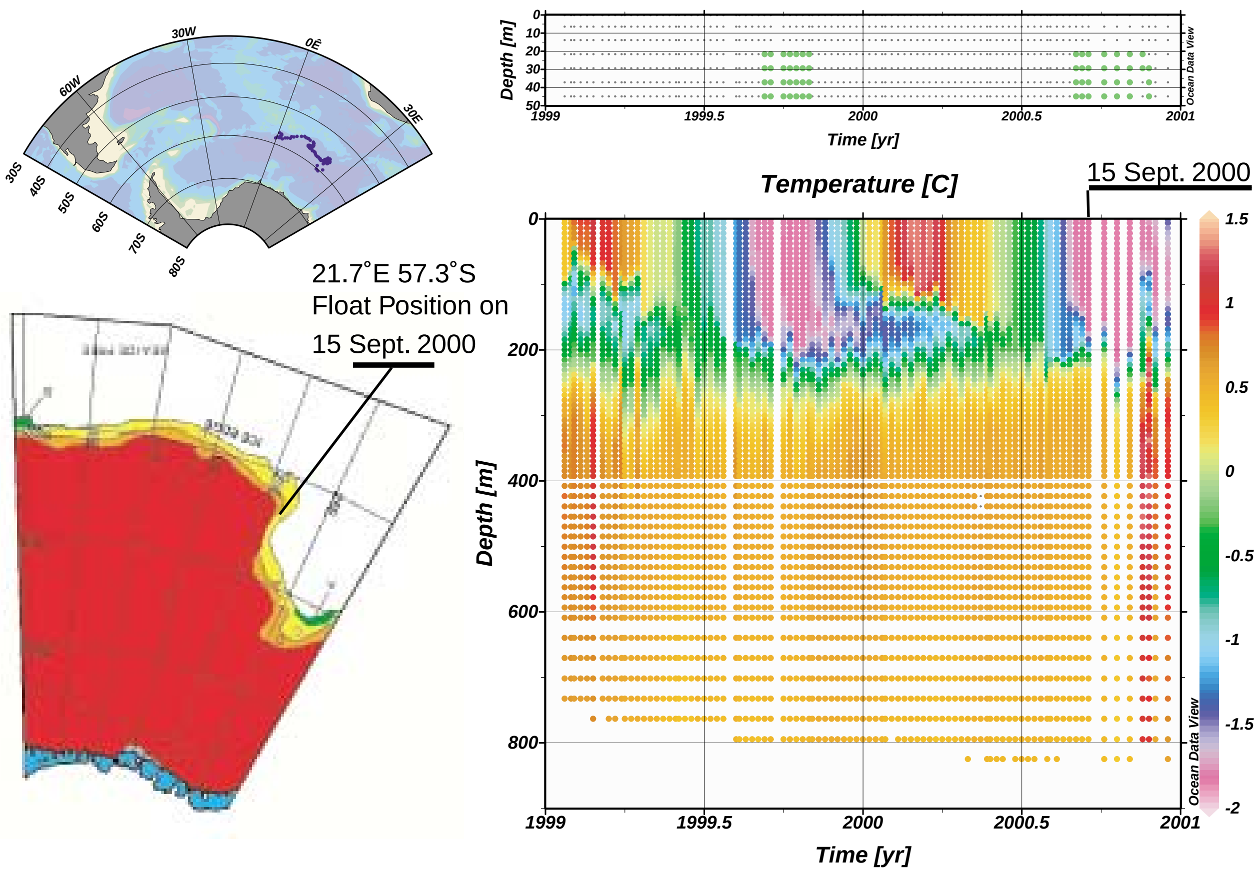

Boebel & Fahrbach *Figure 4*:
Surface positions and temperature profiles of float AWI-08064 and ice coverage in eastern sector of the Weddell Gyre (US National Ice Center, 2001). Ice coverage code: green: 1-3 tenth; yellow: 4-6 tenth; orange: 7-8 tenth; red: 9-10 tenth; gray: fast ice (10 tenth); cyan: ice shelf.

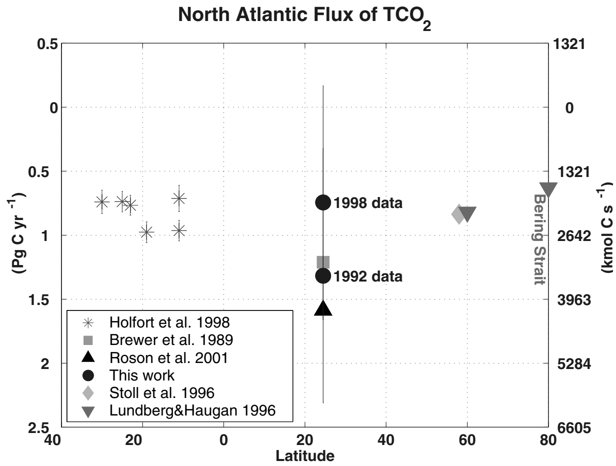

***Figure 1**:*
Carbon transport as a function of latitude in the Atlantic. The Brewer et al. (1989) results shown in this figure have been corrected to include the effect of a net mass transport (Bering Strait and freshwater) through the section. (Adapted from Wallace (2001) and updated with the present results).

and surface values are higher to the south of 24.5°N than to the north (Gruber, 1998). Therefore, the net transport of C_{ANTH} across 24.5°N is strongly affected by the difference in concentrations between the northward flowing shallow Florida Current and the mass balancing return flow dominated by the deep interior. The net northward transport of C_{ANTH} is opposite to the net flow of total carbon and suggests, as has been found by others, that the pre-industrial southward transport of carbon within the Atlantic was stronger than it is today.

Acknowledgements

This research was carried out in part under the auspices of the Cooperative Institute of Marine and Atmospheric Studies (CIMAS), a Joint Institute of the University of Miami and the National Oceanic and Atmospheric Administration, cooperative agreement #NA67RJ0149, and it was also sponsored in part by the National Oceanic and Atmospheric Administration Office of Global Programs and the Office of Oceanic and Atmospheric Research.

References

Battle, M., M. Bender, P. Tans, J. W. C. White, J. T. Ellis, T. Conway, and R. J. Francey, 2000: Global carbon sinks and their variability inferred from atmospheric O_2 and δ13C., Science, 287, 2467-2470.

Brewer, P. G., C. Goyet, and D. Dryssen, 1989: Carbon dioxide transport by ocean current at 25°N latitude in the Atlantic Ocean, Science, 246, 477-479.

Gruber, N., 1998: Anthropogenic CO_2 in the atlantic ocean, Global Biogeochemical Cycles, 12, 165-191.

Gruber, N., J. L. Sarmiento, and T. F. Stoker, 1996: An improved methods for detecting anthropogenic CO_2 in the oceans, Global Biogeochemical Cycles, 10, 809-837.

Hall, M. M., and H. L. Bryden, 1982: Direct estimates and mechanisms of ocean heat transport, Deep-Sea Research, 29, 339-359.

Hellerman, S., and M. Rosenstein, 1983: Normal monthly wind stress over the World Ocean with error estimates, Journal of Physical Oceanography, 13, 1093-1104.

Lee, K., R. Wanninkhof, R. A. Feely, F. J. Millero, and T. Peng, 2000: Global relationships of total inorganic carbon with temperature and nitrate in surface seawater, Global Biogeochemical Cycles, 14, 979-994.

Macdonald, A. M., M. O. Baringer, K. Lee, D. W. R. Wallace, and R. Wanninkhof, 2002: Carbon transport at 24.5°N in the Atlantic, manuscript in preparation.

Rosón, G., A. F. Rios, A. Lavín, and F. F. P. amd H. L. Bryden, 2001: Carbon distribution, fluxes and budgets in the subtropical North Atlantic, Journal of Geophysical Research, submitted.

Schimel, D., I. Alves, M. Heimann, F. Joos, D. Raymond, and T. Wigley, 1996: CO_2 and the carbon cycle, in Climate Change 1995: The Science of Climate Change: Contribution of WGI to the Second Assessment Report of the IPCC, edited by J. Y. Houghton, pp. 65-86, Cambridge University Press, Cambridge.

Siegenthaler, U., and J. Sarmiento, 1993: Atmospheric carbon dioxide and the ocean, Nature, 365, 119-125.

Wallace, D. W. R., 2001: Storage and transport of excess CO_2 in the oceans: the JGOFS/WOCE global CO_2 survey, in Ocean Circulation and Climate, edited by J. Church, G. Siedler and J. Gould, Academic Press, 489-521.

Property (Units)	1998	1992	Roson et al. [2000]	Brewer et al. [1989]
MASS ($10^9 Kgs^{-1}$)	-1.00 ±1.00	-1.11 ±1.08	-1.30 -	-0.8 -
TIC ($PgC\ yr^{-1}$)	-0.74 ±0.91	-1.32 ±0.99	-1.59 ±0.08	-1.21 -
C_{ANTH} ($PgC\ yr^{-1}$)	0.20 ±0.08	0.17 ±0.06	0.23 ±0.08	- -

***Table 1**:*
Meridional fluxes of TIC, mass and C_{ANTH} across 24.5°N. Results of the inverse solution presented here from 1998 and 1992 are compared to the results from previous analyses. The (Brewer et al., 1989) results are corrected to include the effect of a net mass transport (Bering Strait and freshwater) (Wallace, 2001). Positive values are northward.

Oceanic Biogeochemical Fluxes: A summary of the JGOFS portion of the WOCE/JGOFS Transport Workshop, Southampton, June 25—29, 2001.

A. M. Macdonald, R. Wanninkhof[1], M. O'Neil Baringer[1] P.E. Robbins[2] and D. W. R. Wallace[3]
CIMAS, RSMAS, University of Miami, Miami, FL, USA,
[1]NOAA/Atlantic Oceanographic and Meteorological Laboratory, Miami,FL, USA
[2]Scripps Institute of Oceanography, CA, USA.
[3]University of Kiel, Kiel, Germany
amacdonald@whoi.edu

Beginning in the late 1980s and continuing through the decade of the 1990s, the Joint Global Ocean Flux Study (JGOFS) conducted a comprehensive programme to extend our knowledge of the global ocean carbon cycle through the biogeochemistry of the oceans. A main focus of the JGOFS programme was to acquire both the quality and quantity of measurements necessary to identify and quantify biogeochemical processes within the ocean, their interaction with the atmosphere and their influence on, and response to, human-induced perturbations. This goal required international cooperation and collaboration among the physical, chemical and biological disciplines. The programme was comprised of six components: Times series, process studies, a global oceanic CO_2 survey, an ocean colour satellite survey, synthesis and modelling, and data management.

The purpose of the JGOFS component of the Southampton Workshop was to bring together representatives from both the physical and biogeochemical fields in order to: 1) Have a forum for an exchange of ideas among individuals from different disciplines. 2) Assess the present state of knowledge. 3) Recommend a course for future collaborative study of biogeochemistry and circulation within the oceans.

There was a strong focus on the carbon cycle; however, it did not exclude the related cycles of freshwater, heat and nutrients. The international group of attending experts, from eleven different countries, included observationalists and modellers, physical oceanographers, biogeochemists, atmospheric scientists and a mixture of senior scientists, post-docs and students.

The meeting was held as a set of invited plenary talks (see summary below), working group sessions (see recommendations below) and poster presentations (see http://www.woce.org/news/transp_wkshop). The summary and list of recommendations which follow represent an interdisciplinary and international consensus of the communities seeking to better understand ocean biogeochemical fluxes and their influence upon the global carbon system in which we all live.

Plenary Session Summary

The pre-industrial concentration of atmospheric CO_2 was about 280 μatm. At present it is 370 μatm and rising. The release of carbon into the atmosphere through fossil fuel emissions has averaged about 6.2 PgC yr^{-1} over the last decade. Meanwhile, atmospheric CO_2 concentrations have increased at a rate of 2.8 PgC yr^{-1}. Both modelling and pCO_2 studies indicate that the amount of carbon stored in the ocean is increasing by about 2 PgC yr^{-1}. Estimates of land storage remain uncertain. The questions at hand are where are the oceanic sinks of anthropogenic carbon, how big are they and what controls them?

The oceanic and atmospheric carbon budgets are intimately related. Atmospheric carbon isotope inversions are used to identify possible sources and sinks by applying a 'model created' atmospheric transport field to measured distributions of trace gases. Usually the atmospheric carbon and ^{13}C budgets are used to determine the net fluxes of carbon from the ocean and terrestrial biosphere to the atmosphere. From an oceanic perspective such inversions are useful, as they provide an independent estimate of the net carbon entering the ocean.

The coordinated efforts of WOCE, JGOFS and OACES (The Ocean Atmosphere Carbon Exchange Study) have provided thousands of direct measurements of carbon and carbon related properties over the last decade. To make these observations available to the scientific community there has been an organised programme to synthesize these data into a consistent data set (Global Ocean Data Analysis Project). This is now being used to examine ocean transport and global inventories of anthropogenic CO_2

The state of global coarse resolution carbon cycle models is being investigated with the Ocean Carbon Model Intercomparison Project (OCMIP). These models are one of the few tools available for exploring carbon dynamics as they relate to climate change. Comparing the models to each other as well as to the WOCE/JGOFS survey affords an excellent opportunity for understanding the large scale predictive skill they provide, and points to a number of issues which remain unsolved. These models are providing a means to explore how processes which vary regionally work together to produce integrated property fluxes.

As the global carbon survey gives us a "snapshot" of the oceanic carbon concentrations, a few individual locations such as the Bermuda Atlantic Time Series (BATS), in the western North Atlantic, and the Hawaii Ocean Time Series (HOT), in the central North Pacific, are providing detailed time series of the ocean carbon cycle. During the 1990s surface seawater total CO_2 at BATS increased at a rate of 2.2±6.9 μmol kg^{-1} yr^{-1}, while the partial pressure of CO_2 increased at a rate of 1.4±10.7 μatm yr^{-1}. These increases are attributed to the uptake of anthropogenic CO_2 combined with interannual variations in hydrographic properties within the subtropical gyres. Some of this variability can be linked to large-scale climate variations, such as the North Atlantic Oscillation and the El-Nino Southern Oscillation, through a comparison of temporal anomalies. As BATS and HOTS continue to collect data, and as new time series stations are begun, our understanding of how biogeochemistry is influenced by climate variability will improve, as will our ability to predict future changes.

Working Group Recommendations

The working groups (carbon transport, regional budgets and variability, modelling) produced statements summarizing (a) the status of knowledge after the JGOFS field programme, (b) issues still considered crucial for study and (c) recommendations for future collaborative efforts to resolve these issues (WOCE, 2001). Table 1 is an abridged version of the list of working group recommendations associated with observations.

WOCE/JGOFS gave us a single "snapshot" of global ocean circulation. To understand this system in the context of a changing climate this is not adequate. There remains the need to design a system of observations which can resolve temporal changes in large-scale circulation and biogeochemical transports. Table 2 lists those recommendations related to modelling. It was also suggested that further research be conducted into the processes governing the physical and biogeochemical interaction in the interior circulation, the surface mixed layer, frontal regions, topography and the coastal margin, as well as further study of the effects of wind and rivers.

There is a strong recommendation for collaboration amongst CLIVAR and international carbon communities and other biogeochemical programmes. The immediate start of collaboration between the physical and biogeochemical communities for experiment design (including survey lines) is also extremely important, as is collaboration amongst the biogeochemical physical and atmospheric communities in the development of atmosphere/ocean biogeochemical coupled models. If questions are phrased to take advantage of the capabilities of all groups (physicists, biogeochemists, atmospheric scientists), the coordinated effort will be beneficial not only to those involved, but also to the international effort to understand and control anthropogenically caused climate variations.

TABLE 1

Working Group Observation Related Recommendations
Measurement of both spatial and temporal variability in the ocean carbon budget
Exploration of such variability on interdecadal time scales
Measurement of dissolved organic matter, iron, micronutrients and new transient tracers
Standard reference materials for nutrients and metals other than Dissolved Inorganic Carbon and Dissolved Organic Carbon
New technology for measuring biogeochemical properties to take advantage of float, ship of opportunity and other time series programmes should continue to be developed
To improve experiment design and use of resources, fine resolution, regional model simulations in the spirit of the coarse resolution adjoint sensitivity studies would be extremely useful

Acknowledgements

Support for the workshop was provided by U.S. JGOFS, International JGOFS, the Intergovernmental Oceanographic Commission, U.S. WOCE and International WOCE. The US WOCE and US JGOFS surveys were sponsored by the U.S. National Science Foundation in collaboration with the National Oceanic and Atmospheric Administration, the National Aeronautics and Space Administration, the Department of Energy and the Office of Naval Research.

References

WOCE INTERNATIONAL PROJECT OFFICE, 2001 Report of the WOCE/JGOFS Ocean Transport Workshop, Southampton Oceanography Centre, Southampton, UK, 25-29 June, 2001, WOCE Report No. 172/2001, 60 pp.

TABLE 2

Working Group Model Related Recommendations
Further study of the processes which set stoichiometric ratios and study of how the interplay among functional groups effect biogeochemical budgets
New metrics for testing biogeochemical models should be developed
Intercomparison efforts (model/model and model/data) should be continued
Creation of hybrid coordinate models, earth system models (atmos/ocean/biogeo) and inversion toolboxes
Extension of biogeochemical models beyond carbon, and assimilation of biogeochemical data into various types of models

Weddell Sea inflow from floats

Olaf Boebel and Eberhard Fahrbach
Alfred Wegener Institute for Polar and Marine Research, 27515 Bremerhaven, Germany
oboebel@awi-bremerhaven.de

Feeding water to the big chiller

Water masses modified in the Southern Ocean and the Antarctic Circumpolar Current (ACC) form significant components of the global ocean thermohaline circulation (Schmitz, 1995). The global circulation is partly driven by the formation of Antarctic Bottom Water, 66% of which is derived from the Weddell Sea Bottom and Deep Waters (Rintoul, 1998). These water masses are formed by intensive heat loss from the ocean surface to the atmosphere, triggering an increase in density and subsequent sinking of this water (Carmack, 1990). Waters at shallow depths, which drift south from the subtropical gyre to the Antarctic coast, supply this process. The resulting meridional mass and heat transport occurs by two distinctly different processes: a) Through mesoscale eddies which facilitate the transport across the ACC, and b) in the large-scale subantarctic gyres that extend the transport to the Antarctic coast.

The existence and location of the subpolar gyres are directly linked to the transition from westerly to easterly winds over the Weddell Sea. Near the coast the prevailing easterlies cause a westward coastal current (Figure 1). In the region farther offshore the dominant westerly winds force an eastward current, forming the northern leg of the subpolar gyre, which occasionally merges with the ACC. In the western Weddell Sea, the meridional extent of the Antarctic Peninsula causes topographic steering of the oceanic circulation, by which water is guided north as far as 60°S (Fahrbach et al., 1998).

The southward leg of the Weddell Gyre is less well defined. Both the large-scale structure of the wind stress of the Weddell Gyre, as well as topographic features of the Mid-Oceanic-Ridge favour meridional flow components. Such flow would be expected at sub-surface levels only, since the Ekman drift, which overlies the thermohaline circulation, causes a northward flow in the region of the westerlies, a notion confirmed by drifters at the sea-surface or on ice floes, which show no evidence of a southward flow in the eastern Weddell Gyre (Kottmeier and Sellmann, 1996).

Indirect evidence for the southward import of warm Weddell Deep Water is however found in water mass properties. Differences in water mass properties in the Warm Deep Water level between the

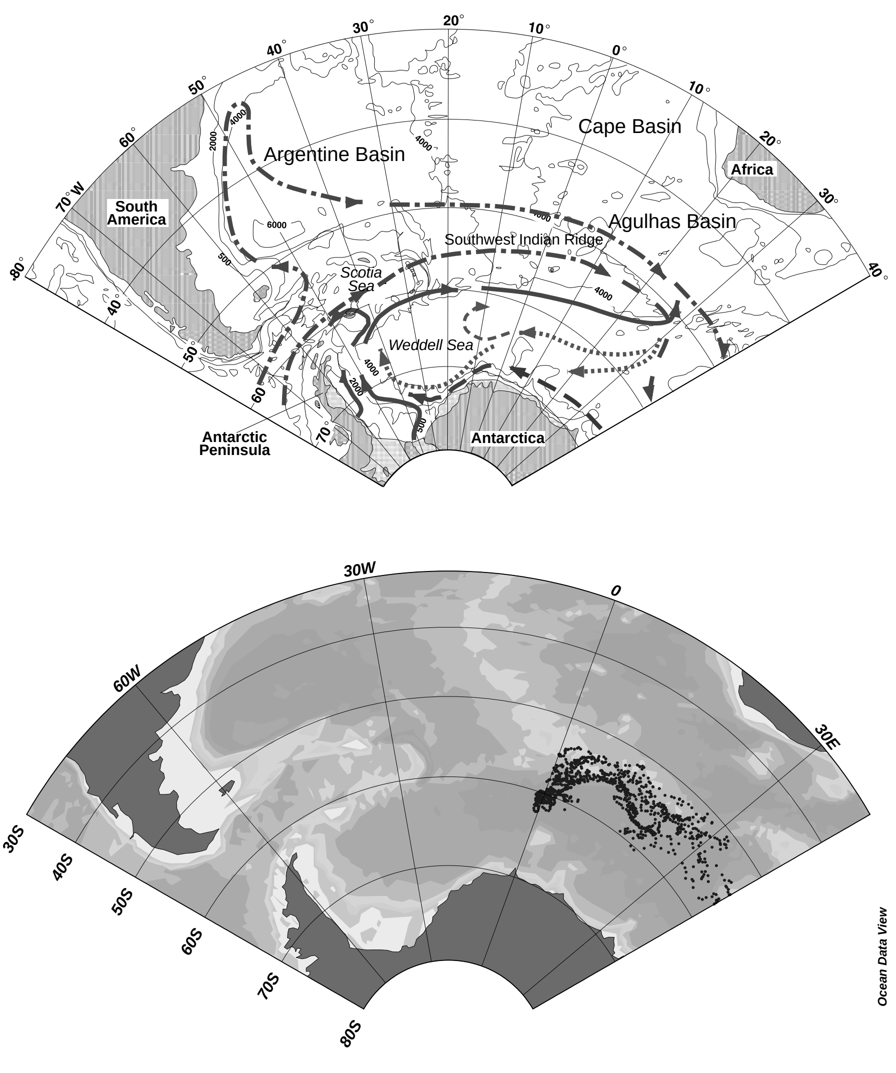

Figure 1:
Top*: Schematic flow diagram in the Atlantic Sector of the Southern Ocean. Arrows indicate warm (dotted) and cold (solid) varieties of Weddell Deep Water, the Antarctic Circumpolar Current (dash-dotted), and the Coastal Current (dashed).* ***Bottom****: Topography and surface positions of profiling PALACE floats deployed by the AWI between 1998 and 2000.*

Figure 2:
Occupation numbers of 2° by 2° boxes (top) and mean velocities from PALACE floats (bottom).

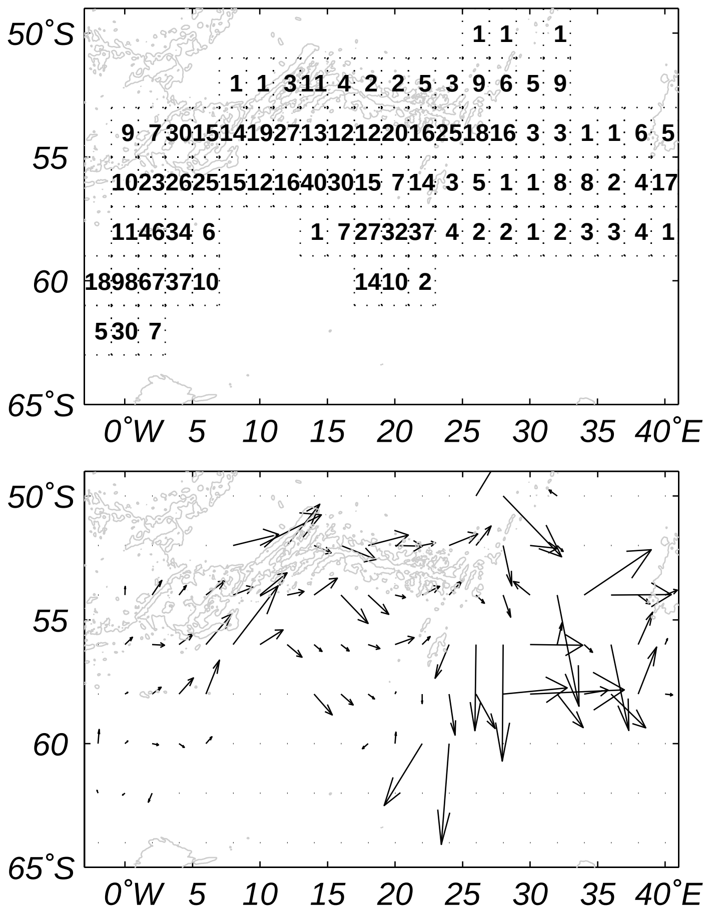

northern and southern part of the Weddell Gyre at the Greenwich Meridian (T> 1°C, S>34.7 near 67°S in contrast to T<0.5°C, S<34.68 at 58°S) necessitate a significant water mass transformation in the eastern Weddell Gyre. New observations (Schröder and Fahrbach, 1999) suggest that the meridional inflow of warm, salty water occurs via mesoscale eddies, which are formed by instabilities of the frontal zone between the ACC and the northern Weddell Gyre. Observations of such eddies were also reported by Gouretski and Danilov (1994) in the eastern Weddell Gyre.

Additional support for such flow patterns exists in recent temporal changes of properties of Weddell Sea Deep Water. Within the Warm Deep Water, the temperature is intermittently rising in the southern half of the section, but decreasing in the northern half. This suggests that Warm Deep Water is injected into the eastern Weddell Gyre and that more Circumpolar Deep Water is entering the central Weddell Gyre from the east than during the past.

First results

To capture the processes behind the Weddell Sea inflow 10 PALACE floats have been launched each austral summer (since 1998) near the Greenwich Meridian between 55°S and 65°S. Latitude and longitude data of weekly float surface positions were interpolated using a spline function and resampled at daily intervals. Zonal and meridional velocities were calculated from the analytical derivatives of the spline's piecewise polynomial form and evaluated at the times of location fixes. Velocity estimates therefore represent tangents along the trajectory, rather then centered differences. Possible contamination of the velocity data through surface drift (Schmid et al., 2001), has been disregarded for now, but will be included in forthcoming detailed analyses. The resulting data set was binned into 2° longitudinal by 2° latitudinal boxes, for which box occupation numbers (estimated number of float weeks in each box), mean velocities, and mean and eddy kinetic energy were calculated.

The floats, generally speaking, drift east in the direction of the ACC. Several instruments, launched near 60°S remain quasi-stationary and soon experience difficulties in reporting back their data via satellite link when the sea-ice starts extending north. Most floats, however, first move away from the approaching sea-ice boundary due to a significant northward component in the mean flow near 60°S 0°E. This result is, in fact, highly reliable, being based on 98 independent 7-day displacement vectors (Figure 2).

To the north, the mean flow appears to follow the Southwest Indian Ridge from 2°E to 24°E (Figure 2). Along the northern flank of the ridge increased levels of mean kinetic energy are observed (Figure 3), telltale signs of the ACC. The ACC's swiftness, however, results in very low occupation numbers in these boxes, making the results statistically insignificant. Most floats drifted south of the Southwest Indian Ridge. Estimates of Eddy Kinetic Energy (EKE) in this region range from 1 to 5 J m^{-3}, a value typical for the intermediate layer of the interior ocean (Boebel et al., 1999). East of 30°E, several vectors pointing south are suggestive of the elusive southward inflow of Circumpolar Deep Water, though statistics here are rather poor and a reliable analysis must await the collection of more data from this area. To collect more data however, we had to first address the issue of possible float – ice interaction, which seems to have significantly reduced the proportion of functioning floats with time.

Technical advances

The analysis of the 30 profiling floats deployed so far attests to a significantly increased failure rate during (partial) ice coverage of the area of operation. This is exemplified here through float AWI-08064 together with a concurrent map of ice-coverage (Figure 4, see page 18). During the winter of 1999 the float only twice failed to report its data and surface position to the satellite, probably due to being trapped under

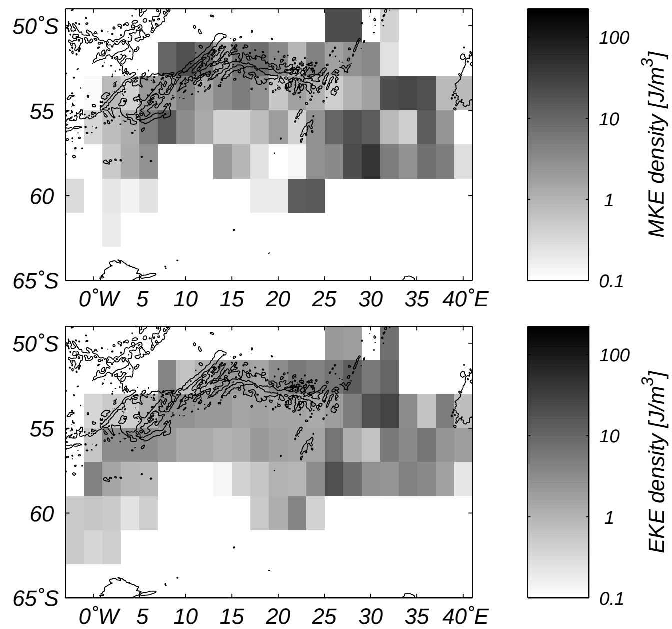

Figure 3: Mean (top) and Eddy (bottom) Kinetic Energy density (MKE and EKE) from PALACE float displacements

the ice. However, in winter 2000, an increase in "missing profiles" was observed (i.e. the white lines in the temperature panel). While succeeding to transmit after 5 such failed surface attempts, the data transmitted by the float indicates a problem in the temperature sensor. Rather unrealistic temperatures are reported at all depths. Shortly thereafter, the float appears to have failed completely and no more transmissions were received.

As shown by Figure 4, at the beginning of the missing transmissions in winter 2000, the float was located near the ice-edge in an area of 50% ice coverage. With time, the ice-edge progressively moved northward. The float, due to the incomplete ice-coverage, was able to surface occasionally. However, being trapped between ice floes, which move in the swell, it is likely to have experienced significant mechanical stress, which we assume caused its final failure.

An analogous correlation between missing profiles and growing ice-coverage was observed for several floats. To increase the average float lifetime of future deployments we, in close cooperation with Webb Research Corporation (WRC), have conceived instrument-based software that acts as an "ice-avoidance" mechanism by aborting the float's ascent at 20 dbar under certain conditions. This mechanism does not detect ice directly, but only conditions favourable to ice-formation, based on the ambient temperature in the upper water column. It therefore is a conservative approach and will abort some profiles, even though no ice is actually present at the surface.

The top right panel of Figure 4 marks (by green dots) those profiles that would have been terminated if this mechanism had been implemented. Clearly, there are green points either side of the "missing profiles". We can therefore assume the missing profiles would also have been terminated and the float would have avoided ice-contact and eventual damage. The new software is currently being tested on five out of nine floats of the WRC APEX type launched in December 2001. Two of these floats have been launched in a partially ice-covered region.

Within the framework of ARGO, we intend to launch more vertically profiling floats across the ACC. In order to extend our studies of the inflow of water into the Weddell Gyre east of the Greenwich Meridian, the floats are programmed to drift at the level of circumpolar deep water. Further technological improvements are planned, such as an interim storage of aborted profiles to transmit the data later when the ice situation is less severe.

References

Boebel, O., C. Schmid, and W. Zenk, Kinematic elements of Antarctic Intermediate Water in the western South Atlantic, Deep-Sea Research II, 46 (1/2), 355-392, 1999.

Carmack, E.C., Large-Scale Physical Oceanography of Polar Oceans, in Polar Oceanography, Part A: Physical Science, edited by W.O. Smith Jr., pp. 171-222, Academic Press Inc., San Diego, 1990.

Fahrbach, S.H. E., G. Rohardt, M. Schröder, and R.A. Woodgate, Flow of bottom water in the northwestern Weddell Sea, Journal of Geophysical Research, 106 (C2), 2761-2778, 2001.

Fahrbach, E., A. Klepikov, and M. Schröder, Circulation and water masses in the Weddell Sea, in Physics of Ice-Covered Seas. Lecture Notes from a Summer School in Savonlinna, Finland 6-17 June 1994, Helsinki University Press, Savonlinna, Finland, 1998.

Gouretski, V.V., and A.I. Danilov, Characteristics of warm rings in the African sector of the Antarctic Circumpolar Current, Deep-Sea Research, 41 (8), 1131-1157, 1994.

Kottmeier, C., and L. Sellmann, Atmospheric and oceanic forcing of Weddell Sea ice motion, Journal of Geophysical Research, 101, 20809-20824, 1996.

Rintoul, S.R., On the origin and influence of Adélie Land Bottom Water, in Oceanology of the Antarctic Continental Shelf, edited by S.S. Jacobs, and R.F. Weiss, pp. 215-240, American Geophysical Union, 1998.

Schmid, C., R.L. Molinari, and S.L. Garzoli, New observations of the intermediated depth circulation in the tropical Atlantic, Journal of Marine Research, 59, 281-312, 2001.

Schmitz, W.J., On the interbasin-scale thermohaline circulation, Reviews of Geophysics, 33 (2), 151-173, 1995.

Schröder, M., and E. Fahrbach, On the structure and the transport in the Eastern Weddell Gyre, Deep-Sea Research II, 46, 501-527, 1999.

US National Ice Center, Antarctic Ice Charts, http://www.natice.noaa.gov, 2001.

Eddies in the western Subarctic Pacific: Their internal structure and linkages to the regime shift phenomena

Konstantin A. Rogachev[*] and Eddy C. Carmack[**]
[*]Pacific Oceanological Institute, Vladivostok, 690041, Russia.
[**]Institute of Ocean Sciences, Sidney, B.C., V8L 4B2, Canada
rogachev@poi.dvo.ru

1 Introduction

Large anticyclonic eddies form at the confluence of the Kuroshio and Oyashio currents and then migrate northeastward into subarctic waters along the full length of the Kuril-Kamchatka Trench. Such eddies play an important role in the mixing of subtropical and subarctic waters. Of particular interest is the fact that each large eddy has a well-mixed core, thus facilitating the vertical supply of nutrients to the upper layer.

Significant temporal variability has been observed in the subarctic Pacific during the last decade. This variability may be compared with the regime shift that occurred in 1976-1978. These observations show that there was thermohaline transition in the western subarctic boundary currents in 1990-1997. Upper layer temperature decreased, while stratification and the strength of the coastal Oyashio increased during this transition. The unique time series of observations in the Oyashio allows one to find the new index of rapid climatic changes in the ocean – thermohaline features of the large anticyclonic eddies in the western boundary currents. During thermohaline transition to strong stratification, the horizontal and vertical sizes of the Oyashio eddies decreased, while their dynamic height dropped. New observations in the year 2000, show that during four years the boundary currents returned to the state with large and deep Oyashio eddies, and with high dynamic topography.

In autumn 1990, a cooperative study of circulation in the Subarctic Western Pacific (the INPOC study) was carried out by the Pacific Oceanological Institute (Russia) and the Institute of Ocean Sciences (Canada) aboard the *RV AKADEMIK VINOGRADOV*. As part of the Canadian WOCE Program, 3 ARGOS surface drift buoys were deployed in the Oyashio region (Fig. 1). Each buoy had a drag sail 6 m in length and 1 m in diameter, positioned at a depth of about 15 m. The three buoys were released on a section across the center of so-called eddy WCR86B on November 6, 1990. At the same time an XBT section to a depth of 800 m was carried out during the deployment of the drifters.

Figure 1
Map of the study area (a) and the second bouy track in November-December 1990 (b).

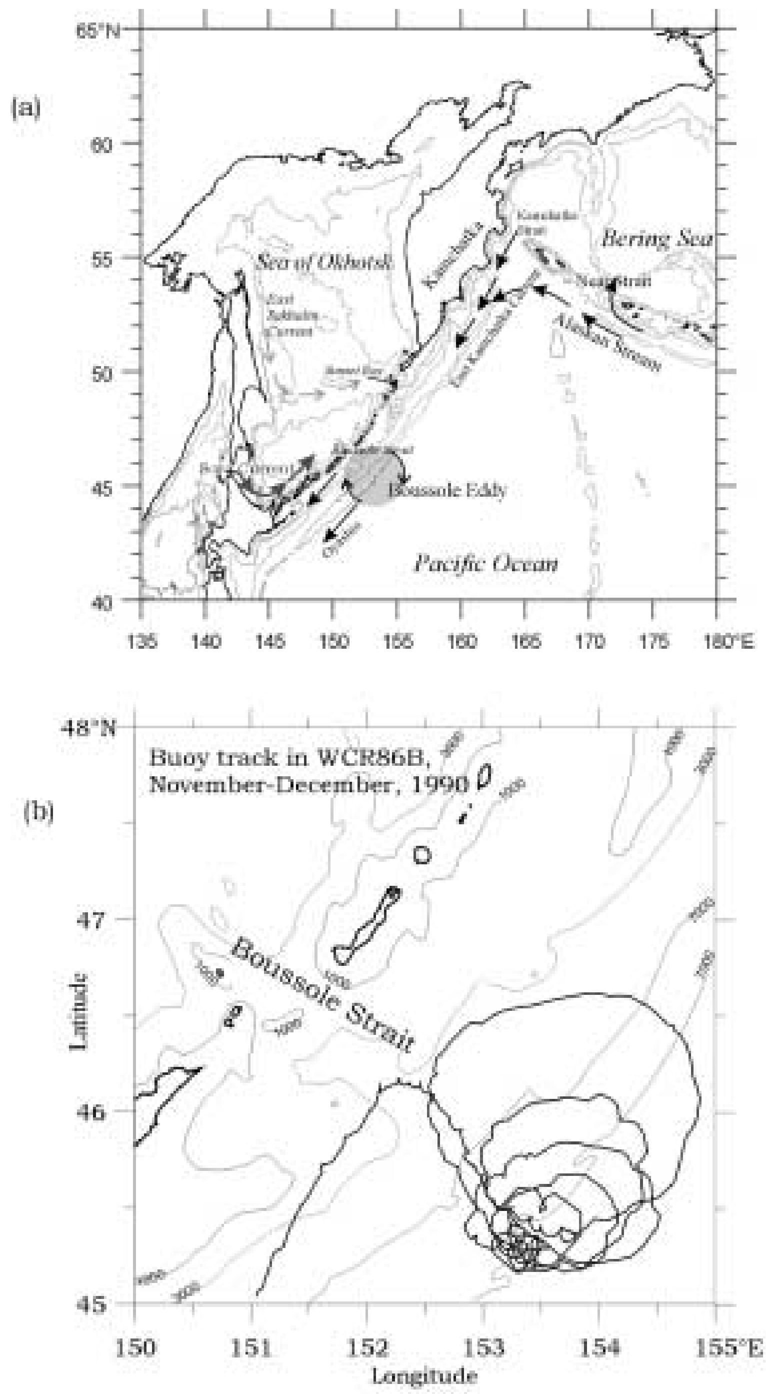

The 1990 eddy was the largest eddy observed during recent decade from 1990 to 2000 off Boussole Strait (Rogachev and Carmack, in preparation; Rogachev and Lobanov, 2001).

In the present work we use the tracks of ARGOS drift buoys deployed in an anticyclonic ring WCR86B to show that (a) large amplitude, near-inertial waves are observed in the region of negative relative vorticity associated with an Oyashio ring, and that (b) the effective frequency of near inertial waves are locally decreased to values near that of diurnal tides.

Here we report on one buoy deployed within WCR86B that shows evidence of large amplitude, near-inertial motions. During its first week within the eddy the buoy drifted with a mean azimuthal current speed of 0.40-0.45 m s^{-1}, and a radius of rotation of 15-20 km. Superimposed on the mean rotation of the eddy were near-diurnal period loops of radius 7-8 km. During successive rotations the buoy spiraled outward, its mean period of rotation increased, and the amplitude of inertial motions decreased.

Two explanations for the high-amplitude motions are offered. First, that the relative vorticity of the eddy itself shifts the lower bound of the inertial wave band from the Coriolis frequency to an effective Coriolis frequency, allowing low-frequency near inertial waves to become trapped. We suggest that the possible mechanism, which generates this diurnal motions, along with wind, can be connected with tides. The presence of the anticyclonic eddy and the proximity of the Boussole Strait raises the possibility that these oscillations are eddy-trapped near-inertial waves rather than topographic waves. There is a frequency minimum for near-inertial waves inside the eddy. This frequency minimum produces zero group velocity, which allows amplification of the waves. Wave trapping and amplification can thus occur at the base of the eddy's core. Such amplification should lead to instability and shear production of turbulence so that the rate of mixing should vary with external forcing, e.g. being greatest during the spring tide. Second, that wind-force perturbations may be trapped and amplified within the vortex of the eddy. These conclusions rely on the interpretation of dissipation measurements and eddy spin-down, since production of turbulence can be from external forcing rather than internal instabilities.

2 Results

A horizontal map of dynamic height (0/1000 dbar) shows the location of eddy WCR86B off Boussole Strait. Its diameter is seen to be about 200 km (Fig. 1a and 1b). The internal structure of the eddy is marked: (a) By the downward bending of isotherms, (b) by a shallow subsurface core of relatively warm water ($T > 3^{o}C$) between 100 - 300 m and (c) by an underlying core of colder water ($T < 2^{o}C$) between 200 - 700 m. Cold and warm cores encircle the eddy's perimeter at intermediate depths. This section shows that first buoy was deployed at western edge of the eddy, second buoy near its center, and the third buoy at its eastern edge. In the following discussion we will focus on the behaviour of the second buoy.

The buoy track (Fig. 1b) shows two kinematic properties: The large-scale anticyclonic rotation around the eddy (circuit) and the smaller-scale anticyclonic rotations on the eddy's perimeter (loops). The mean azimuthal current speed changed depending on the position of the buoy relative to eddy's centre. For example, the buoy spiraled outward from the eddy's centre making 5 full circles of increasing radius during a period of 40 days. The mean period of rotation of the buoy during the 4 rotations varied from 4 days for the first, 5.5 days for the second, 8.4 days for the third and 9.3 days for the fourth. For convenience, in the analysis below we define from this data a "standard" circuit, which is simply the first full circuit of the buoy around the perimeter of the eddy (Fig. 2a).

Especially pronounced oscillations were observed during the first seven days that the buoy spiraled within the core of eddy (Fig. 2b). The period of oscillation at this time was about 1 day, close to the diurnal frequency (the buoy made 4 inertial loops during 4 days of first circle and 4 loops during the standard circuit). We also note that the highest amplitude motions were observed during the time of spring tides in the area, in the present case at least. However, further observations of fortnightly cycles will be required to confirm this relationship.

3 Discussion

An approximate dispersion relation is derived for the spiral near-inertial waves. There is a frequency minimum, which is less than the effective Coriolis frequency f_{eff} and produces a zero group velocity. The effective Coriolis frequency $f_{eff} = f + 2\Omega$ in a case of solid body rotation. The effective Coriolis frequency replaces the planetary value f as the limiting frequency.

It is well known that strong storms induce inertial currents in the ocean. Inertial motions after passage of storms have been detected by moored current meters and drifting buoys (Pollard, 1970; Tomosada, 1991; Taira et al., 1993).

The tidal generation mechanism considered here is a hypothesis, since we do not resolve enough fortnightly cycles to support the contention that high-amplitude near-inertial oscillations are tide rather than wind generated. As far as evidence presented in this paper goes, it is as likely that the inertial oscillations are generated by the passage of an atmospheric front. Therefore, wind generation should be given equal exposure. However, all the strong atmospheric storms cited above forced much weaker inertial motions compared with our case. Thus the generation mechanism of these high-amplitude oscillations should be stronger than those generated by an atmospheric front.

Figure 2.
Path of the bouy in the first circuit (a) and radial and azimuthal velocity deviations (cm/s) in the first and standard circuits (b).

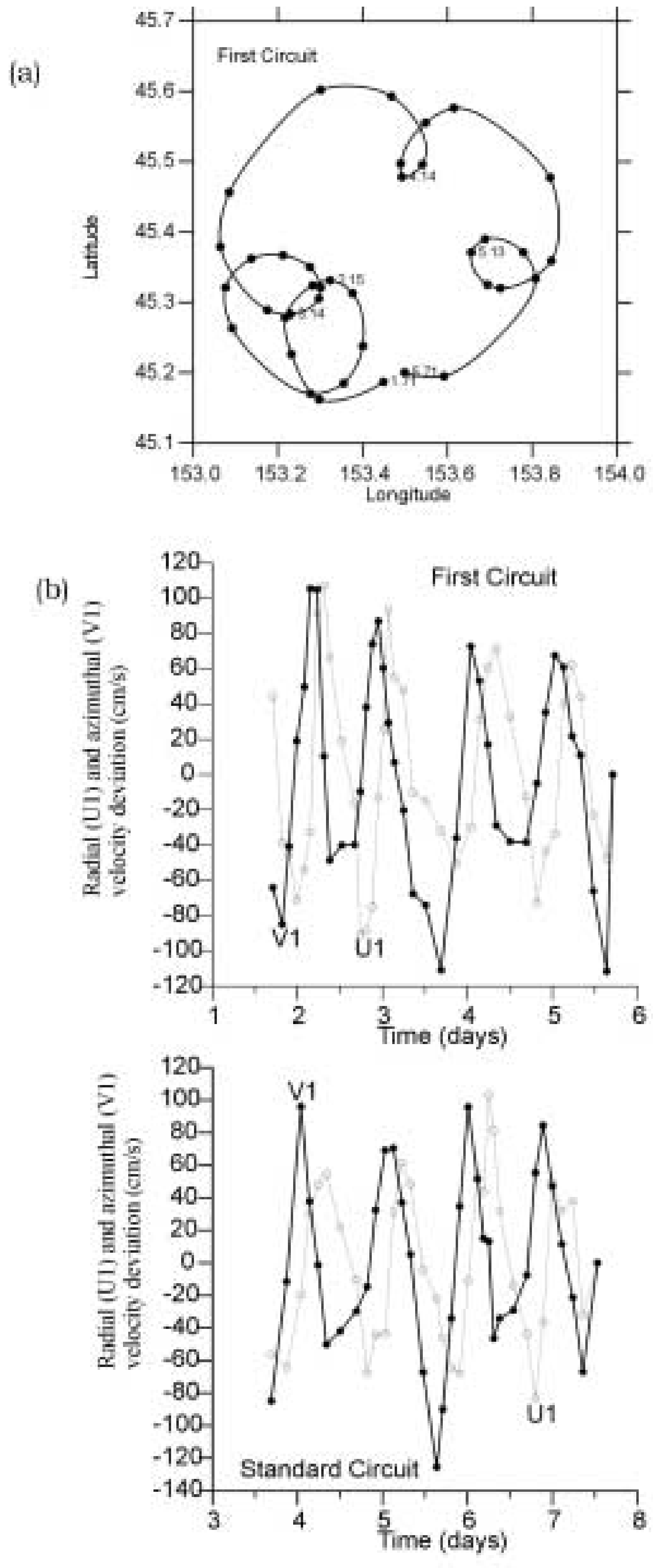

A tidal flow over the Boussole Strait sill excites internal waves. Strong tidal currents are observed within the Boussole Strait (Thomson et al., 1997). Tidal currents generate internal waves at tidal frequencies. Numerical experiments (Nakamura et al., 2000) show that internal waves at the K_1 tidal frequency are confined to the sill slopes, because the K_1 tide is subinertial in the Kuril Straits. These topographically trapped waves are efficiently generated and contribute to strong tidal currents with maximum amplitude of over 1.5 m s^{-1} in the Kuril Straits. The energy radiated by such waves is a loss of energy from the earth-moon system, but is a major source for mixing in the deep ocean. Internal waves radiate into the ocean interior off the strait and its sill in the form of internal wave rays. Direct observations show the packet of long internal waves (Rogachev et al., 1996), which propagates eastward from Kuril Straits (Boussole and DeVries). It is important that these waves are observed simultaneously with high-amplitude inertial oscillations revealed by drifters. The pronounced cross-slope transport (volume flux) is the most important factor determining internal tide generation. We may expect that the strait region is the principal site for the conversion of barotropic tidal energy into baroclinic tides. Recently (Cummins et al., 2001) showed that the Aleutian Pass is one of the important region for baroclinic energy conversion.

4 Conclusions

This paper presents an analysis of current observations of a large Oyashio anticyclonic eddy. A striking feature of these observations is the relatively strong diurnal currents inside the eddy core. This strong amplification of diurnal currents is absent further outside the eddy core. With a simple model it is shown that this amplification can be explained by inertial wave trapped inside the extremely large and low-stratified eddy. Waves starting in the negative vorticity trough will have frequencies below the effective local inertial frequency outside this region, so they will not be able to propagate freely away.

The extremum in the dispersion relation corresponds to zero group velocity, so energy cannot escape the region. A kind of resonance takes place. This type of resonance does not occur for diurnal frequency outside the eddy.

The local planetary inertial period was less than the observed period of these motions. A sharp increase of the near inertial period was detected in the core of the Oyashio eddy. We suggest that the change of inertial period is due in part to relative vorticity created by the eddy. The effective inertial period is very near to the diurnal. The contribution of relative vorticity to the dispersion relation of near-inertial waves is near that required to reduce the lower bound of near-inertial waves to diurnal frequency. Hence, the possibility exists that the inertial motions were set up by the strong tidal influence. The results described here suggest that tidal forcing can be considered as a possible mechanism for generation of the inertial motions along with the wind forcing. With the limited data available we cannot distinguish between temporal variability induced by the fortnightly tidal cycle and spatial variability associated with vortex-trapped waves, which will evanesce outside the velocity maximum, and thus, could equally well be generated by wind-forcing.

Despite that the exact mechanism for the inertial wave generation is not yet clear, the large-amplitude near-inertial waves are probably responsible for the formation of the well-mixed core of an anticyclonic eddy and therefore may play essential role in water mass transformation in the region.

Acknowledgements

Professor P.H. LeBlond is gratefully acknowledged for making available the drifters which we successfully deployed in the largest Oyashio eddy, in 1990, during the implementation of two Russia-Canada projects: INPOC and WOCE.

References

Cummins P. F., J. Y. Cherniawskiy, and M. G. G. Foreman, 2001: North Pacific internal tides from the Aleutian Ridge: altimeter observations and modeling. J. Marine Research, 59(2), 167-191.

Nakamura T., T. Awaji, T. Hatayama, K. Akitomo, T. Takizawa, T. Kono, Y. Kawasaki, M. Fukasawa, 2000: The generation of large-amplitude unsteady lee waves by subinertial K1 tidal flow: A possible vertical mixing in the Kuril Straits. J. Phys. Oceanogr., 30, 1601-1621.

Pollard R. T., 1970: On the generation by winds of inertial waves in the ocean. Deep-Sea Research, 17, 795-812.

Rogachev K. A., A. S. Salomatin and E. C. Carmack, 1996: Concentration of pelagic organisms at mesoscale fronts in the western subarctic Pacific: small fish on long waves. Fisheries Oceanography, 5, 153-162.

Taira K., S. Kitagawa, H. Otobe and T. Asai, 1993. Observation of temperature and velocity from a surface buoy moored in the Shikoku Basin (OMLET-88)- An oceanic response to a typhoon. J. Oceanogr., 49, 397-406.

Thomson R. E., P. H. LeBlond, and A. B. Rabinovich, 1997: Oceanic odyssey of a satellite-tracked drifter: North Pacific variability delineated by a single drifter trajectory. J. Oceanography, 53, 81-87.

Tomosada A., 1991: Decay of inertial oscillation observed by ARGOS drifting buoy. Set of papers from the research project “Oyashio Region”. -Bull. Hokkaido Nat. Fish. Res. Institute, no.55, 115 124.

WOCE and Beyond - Planning for the final WOCE Conference

John Gould[1], Carl Wunsch[2], Worth Nowlin[3], Piers Chapman[3]
[1]WOCE IPO, Southampton Oceanography Centre, Southampton UK.
[2]Massachusetts Institute of Technology, Cambridge, MA, USA
[3]US WOCE Office, Texas A&M University, College Station, TX, USA
wjg@soc.southampton.ac.uk

When you receive this Newsletter the final WOCE Conference will be about 10 months away. Here is a review of where we stand and an indication of what you can expect.

The tentative programme (pages 29 and 30).

After much discussion, the organising committee decided to structure the conference loosely around the main scientific objectives of WOCE as they were agreed in the 1980s. Each day will have a general theme that will be addressed by plenary talks in the mornings and by posters in the afternoon sessions. All the posters will be available for viewing from Monday to Thursday, along with afernoon talks with regional foci. Each plenary speaker will be invited to work with a small team of specialists in their particular subject area. They will be asked to identify appropriate material so that each plenary talk will be as wide-ranging as possible. The titles of the plenary talks may not be exactly as they appear in the programme here.

The talks when taken together will highlight the enormous strides that have been taken during the 1990s to make oceanography a much more quantitative science to help us to better understand the role of ocean circulation in the Earth’s climate.

Funding and financial arrangements

In parallel with the programme planning, the US and International WOCE Project Offices have been seeking sponsorship for the conference. We have received commitments from WCRP, from SCOR, IOC, and from the US agencies NSF, ONR, NASA, DOE and NOAA. There are already some commitments to sponsorship from a number of commercial organisations.

This sponsorship will be used to broaden international participation and to subsidise attendance by young scientists and students. To further attract this audience, the registration fee is reduced considerably for students and for early registrants. To encourage poster submissions, there is no poster fee.

The venue

San Antonio has a long history. Spanish explorers and missionaries came to the area in 1691, and because it was the feast day of St. Anthony, they named the river "San Antonio." The city was founded in 1718 when the Mission San Antonio de Valero was established. The mission became known as "The Alamo" when, in 1836, 189 defenders held it for 13 days against some 4,000 Mexican troops. The cry "Remember the Alamo!" became the motto of the Texan revolution against Mexico. The Alamo remains in the heart of the modern city.

The Conference is in the Henry B Gonzalez Convention Center that is also located downtown and will provide excellent facilities for the meeting. Average daily maximum temperatures are in the mid-20s°C.

Registration

The web site for online registration should be available by mid January. http://www.WOCE2002.tamu.edu.

An invitation

This Conference will provide a meeting point for all those who have made a contribution to the project. Furthermore, it will provide a window on WOCE's achievements for the many agencies around the world that have funded the project. It will also be a starting point for the post-WOCE era, providing the scientific community with the opportunity to meet both formally and informally to discuss how we can build on our achievements.

We encourage you to come along and to bring your students and young colleagues, and to submit posters highlighting the exciting work you have accomplished during the WOCE Programme.

Provisional Program

Note that times indicated for presentations include ten minutes for questions and discussion.

Sunday 17 November, 2002

1400-1800 Registration desk open at the Conference Center. Posters may be put up.

1800-1930 Conference Reception, St. Anthony Hotel

Monday 18 November 2002

Theme: New global perspectives, addressing "What were our observational capabilities in 1980? What are they now and how has WOCE helped? What might be our capability in 2010? In 2050?" Quantitative description is requested.

0830-0900 Conference opening and welcome

0900-0930 "Why did we do WOCE?"

0930-1020 "New views of the ocean from space"

1020-1050 Coffee

1050-1130 "The inferred three-dimensional velocity field"

1140-1220 "New technologies: What WOCE developed and what the future might hold?"

1220-1310 "New insights from ocean models"

1310-1430 Lunch

1430-1800 Posters

1600-1700 Review talk: "The Indo-Pacific Oceans"

Tuesday 19 November

Theme: What are the oceans' roles in property transports and exchanges with the atmosphere?

0830-0910 "Ocean transport of heat and freshwater—How good are our estimates? Has WOCE changed the values and uncertainties?"

0920-1010 "Ocean ventilation and water mass conversion rates"

1010-1040 Coffee

1040-1130 "Ocean storage and transport of carbon—its role in global change projections. Tracer analogs"

1130-1220 "Ocean exchanges with the atmosphere—mechanical, chemical, and physical"

1220-1310 "Global synthesis. How far have we come? How far might we get?"

1310-1430 Lunch

1430-1800 Posters

1600-1700 Review Talk: "The North Atlantic Ocean"

Wednesday 20 November

Theme: What insights has WOCE produced regarding how the ocean works and what are the remaining problems?

0830-0920 "Ocean mixing and Energetics - Where? How? Who cares?"

0920-1010 "Boundary currents and interbasin flows. Indicators of the oceans' state?"

1010-1040 Coffee

1040-1130 "Do simplified (two-dimensional/coarse resolution/reduced physics) models have any useful predictive skill?"

1130-1220 "The ocean mesoscale—Is it important for climate?"

1220-1310 "Interaction of ocean biology and climate"

1310-1430 Lunch

1430-1800 Posters

1600-1700 Review Talk: "The Southern Ocean"

Evening: Conference Dinner

Thursday 21 November

Theme: What do we know about the ocean's role in climate, and what are the next main objectives?"

0830-0920 "Climate stability and instability—transition from flywheel to driver"

0920-1010 "Tropical-Intertropical interactions, including ENSO"

1010-1040 Coffee

1040-1130 "What do the large-scale atmosphere/ocean modes of variability imply about memory and predictability?"

1130-1220 "Sea level rise—can we explain what we measure?"

1220-1310 "The ocean component of coupled climate models—What parameterizations and resolutions are needed and how do they vary with time scale?"

1310-1430 Lunch

1430-1800 Posters

1600-1700 Review Talk: "The South Atlantic Ocean"

Friday 22 November

Theme: Beyond WOCE—Where do we go from here?"

0830-1010 "What has WOCE told us should be measured globally/continuously/indefinitely/sporadically/once/regionally? How do we know that?"

1010-1040 Coffee

1040-1120 "After WOCE what are the remaining challenges and how should we set about meeting them?

1200 Closing. Summary of Conference and Outlook..

Dynamics of Overflow Mixing and Entrainment Project invites community participation.

Dense overflows play an important role in supplying water-masses formed in marginal seas to the larger ocean circulation, yet they are typically poorly represented in global ocean models. Recently, several improvements to the parameterisation of overflow mixing processes have been developed. With the aim of assessing these parameterisations and the models they are embedded in, we have formed the Dynamics of Overflow Mixing and Entrainment (DOME) working group. This is a collaboration between several different groups in the US and Europe, including modellers using z-grid, isopycnal and sigma-coordinate models, as well as others familiar with observations of overflows. (A complete list of current participants can be found on the DOME webpage http://www.rsmas.miami.edu/personal/tamay/DOME/dome.html).

There have been two workshops so far, at which we shared progress in understanding overflows, and discussed plans for collaboration.

As a result of these discussions, we have agreed on a model assessment which will be carried out in three stages: Phase I consists of carefully controlled idealized overflow simulations, Phase II consists of more realistic simulations of specific overflows and detailed comparison with observations of these overflows, and Phase III assesses the role of the overflows in global simulations.

Phase I is now underway, and we would like to invite all interested members of the physical oceanography community to participate. We have drawn up a suite of 14 different numerical experiments consisting of 7 different specifications of physical parameters and 2 different horizontal resolutions, although individual participants are free to add more.

Details of the suite of experiments are available from the DOME webpage. Results from only a few of these cases would still be useful, provided at least one of the calculations is the “Base case” described in the document. We also encourage comparison with laboratory experiments and theoretical predictions in Phase I. In order to coordinate the comparison of results, we have agreed to complete our simulations by April 1st. Anyone who plans to meet this deadline should inform Bob Hallberg by March 1st (although we encourage them to contact us for details and perform preliminary experiments well before that date). We stress that this is not a model “beauty contest” but rather an opportunity to identify the characteristics of different models, identify areas ripe for improvement, and focus on the following physical questions: (1) Where and how does entrainment occur? (2) What is the route taken by dense water down the slope?

For further information contact Tamay Ozgokmen (tamay@rsmas.miami.edu), Bob Hallberg (rwh@gfdl.noaa.gov) or Sonya Legg (slegg@whoi.edu).

MEETING TIMETABLE 2002

Feb 11-15	AGU 2002 Ocean Sciences	Honolulu, USA
Mar 27-29	Tracers in Physical Oceanography	Univ. Washington, Seattle, USA
Apr 22-26	EGS XXVII General Assembly	Nice, France
May (TBA)	Working Group on Ocean Model Development	Hamburg, Germany
May 28 - June 1	AGU 2002 Spring Meeting	Washington DC, USA
*Nov 18-22	WOCE FINAL CONFERENCE (www.WOCE2002.tamu.edu)	San Antonio, Texas, USA

*Denotes International WOCE Meeting

The WOCE International Newsletter is published by the WOCE International Project Office.

Editor:
Mike Sparrow

Compilation and layout:
Jean Haynes

The International WOCE Newsletter is distributed free-of-charge upon request thanks to the funding contributions from France, Japan, UK, and WCRP.

This Newsletter provides a means of rapid reporting of work in progress related to the Goals of WOCE as described in the WOCE Scientific and Implementation Plan.

Requests to be added to the mailing list and changes of address should be sent to:
WOCE IPO
Southampton Oceanography Centre
Empress Dock
Southampton SO14 3ZH
United Kingdom
Tel. +44 23 8059 6789
Fax. +44 23 8059 6204
e-mail: woceipo@soc.soton.ac.uk

Contents of past issues together with the electronic PDF version can be found at: http://www.woce.org/publications/newsletters/index.html

Articles, letters, announcements and reviews are welcome and should be addressed to the editor. (mdsp@soc.soton.ac.uk)

Printed by Technart Ltd.
Southern Road
Southampton SO15 1HG
United Kingdom.

If undelivered please return to:

WOCE IPO
Southampton Oceanography Centre
Empress Dock
Southampton SO14 3ZH
United Kingdom.

CONTENTS OF THIS ISSUE